4-2020

A Critical Review of the $^{15}N_2$ Tracer Method to Measure Diazotrophic Production in Pelagic Ecosystems

Angelicque E. White

Julie Granger

Corday Seldon
Old Dominion University

Mary R. Gradoville

Lindsey Potts

See next page for additional authors

Original Publication Citation

White, A. E., Granger, J., Selden, C., Gradoville, M. R., Potts, L., Bourbonnais, A., ... & Tobias, C. R. (2020). A critical review of the $^{15}N_2$ tracer method to measure diazotrophic production in pelagic ecosystems. *Limnology and Oceanography: Methods*, *18*(4), 129-147. doi:10.1002/lom3.10353

LIMNOLOGY and OCEANOGRAPHY: METHODS

ASLO

Limnol. Oceanogr.: Methods 18, 2020, 129–147

doi: 10.1002/lom3.10353

A critical review of the $^{15}N_2$ tracer method to measure diazotrophic production in pelagic ecosystems

Angelicque E. White,[1] Julie Granger,[2]* Corday Selden,[3] Mary R. Gradoville,[4] Lindsey Potts,[2] Annie Bourbonnais,[5] Robinson W. Fulweiler,[6] Angela N. Knapp,[7] Wiebke Mohr,[8] Pia H. Moisander,[9] Craig R. Tobias,[2] Mathieu Caffin,[1] Samuel T. Wilson,[1] Mar Benavides,[10] Sophie Bonnet,[10] Margaret R. Mulholland,[3] Bonnie X. Chang[11,12]

[1]Department of Oceanography, University of Hawai'i at Manoa, Honolulu, Hawaii, USA
[2]Department of Marine Sciences, University of Connecticut, Groton, Connecticut, USA
[3]Department of Ocean, Earth, and Atmospheric Sciences, Old Dominion University, Norfolk, Virginia, USA
[4]Ocean Sciences Department, University of California Santa Cruz, Santa Cruz, California, USA
[5]School of the Earth, Ocean and Environment, University of South Carolina, Columbia, South Carolina, USA
[6]Department of Earth and Environment and Department of Biology, Boston University, Boston, Massachusetts, USA
[7]Department of Earth, Ocean, and Atmospheric Science, Florida State University, Tallahassee, Florida, USA
[8]Department of Biogeochemistry, Max Planck Institute for Marine Microbiology, Bremen, Germany
[9]Department of Biology, University of Massachusetts Dartmouth, North Dartmouth, Massachusetts, USA
[10]Aix Marseille Univ., Université de Toulon, CNRS, Marseille, France
[11]Joint Institute for the Study of the Atmosphere and Ocean, University of Washington, Seattle, Washington, USA
[12]Pacific Marine Environmental Laboratory/NOAA, Seattle, Washington, USA

Abstract

Dinitrogen (N_2) fixation is an important source of biologically reactive nitrogen (N) to the global ocean. The magnitude of this flux, however, remains uncertain, in part because N_2 fixation rates have been estimated following divergent protocols and because associated levels of uncertainty are seldom reported—confounding comparison and extrapolation of rate measurements. A growing number of reports of relatively low but potentially significant rates of N_2 fixation in regions such as oxygen minimum zones, the mesopelagic water column of the tropical and subtropical oceans, and polar waters further highlights the need for standardized methodological protocols for measurements of N_2 fixation rates and for calculations of detection limits and propagated error terms. To this end, we examine current protocols of the $^{15}N_2$ tracer method used for estimating diazotrophic rates, present results of experiments testing the validity of specific practices, and describe established metrics for reporting detection limits. We put forth a set of recommendations for best practices to estimate N_2 fixation rates using $^{15}N_2$ tracer, with the goal of fostering transparency in reporting sources of uncertainty in estimates, and to render N_2 fixation rate estimates intercomparable among studies.

Dinitrogen (N_2) fixation, the biologically mediated reduction of atmospheric N_2 gas to ammonium, is the dominant source of reactive nitrogen (N) to the global ocean (Gruber and Sarmiento 1997; Codispoti 2007; Gruber 2008). N_2 fixation plays a critical role in both the N and carbon (C) cycles by relieving N-limitation of phytoplankton populations and thus enabling carbon dioxide (CO_2) drawdown in the surface ocean (Mahaffey et al. 2005). Over the past century, substantial efforts have been made to characterize the spatial and temporal variability of N_2 fixation rates in the ocean as well as the diversity and biogeography of N_2 fixing organisms (diazotrophs). Nevertheless, considerable uncertainties remain regarding the global magnitude of marine N_2 fixation rates, as well as the chemical, physical, climatological, and ecological factors that control the growth and distributions of marine diazotrophs in the ocean. In particular, the global ocean flux of newly fixed N remains uncertain, in part because N_2 fixation rate estimates derive from various protocols that introduce different levels of uncertainty to estimates, the magnitude of which is seldom reported or considered.

*Correspondence: julie.granger@uconn.edu

Additional Supporting Information may be found in the online version of this article.

The most common method used to estimate marine N_2 fixation rates, first conducted in the Sargasso Sea almost six decades ago (Dugdale et al. 1959), involves tracing the incorporation of stable isotope-labeled N_2 gas ($^{15}N_2$) into particulate matter. This incubation-based approach was later refined by Montoya et al. (1996), who outlined a clear set of methodological procedures that included a template for calculating detection limits and a basis for assessing the sensitivity of the calculation to most sources of analytical and experimental error. The relative ease of this method, increased access to mass spectrometers, and a growing appreciation of the biogeochemical significance of N_2 fixation (Capone and Carpenter 1982) led to thousands of rate measurements spanning the global ocean (*see* Luo et al. 2012). These measurements have been exploited by the oceanographic community to estimate contributions of N_2 fixation to the export of C from the euphotic zone, to construct global ocean estimates of new N inputs via diazotrophy, and to detect basin-scale changes in the N_2 fixation rates (e.g., Karl et al. 2001; Luo et al. 2012).

In recent years, some assumptions inherent to the $^{15}N_2$ assay have been questioned, prompting a re-examination of the method's foundational principles and limitations (Mohr et al. 2010). Methodological refinements have been developed to address some of these limitations (e.g., Klawonn et al. 2015; discussed in depth below), which have led to divergences in experimental approaches among research groups. The variable practices among researchers in certain aspects of the method currently preclude robust comparison of rate estimates across studies, and bias the extrapolation of global-ocean fluxes from rate compilations. The lack of methodological uniformity is concerning in light of a growing appreciation that the activity of diazotrophs is more geographically widespread, and potentially more variable in time and space, than previously considered. The paradigm that diazotrophs are confined to warm, well-stratified oligotrophic tropical and subtropical surface waters has been challenged by reports of N_2 fixation in the aphotic mesopelagic (e.g., Bonnet et al. 2009; Hamersley et al. 2011; Benavides et al. 2015), nutrient-rich coastal zones, (e.g., Grosse et al. 2010; Mulholland et al. 2012, 2019; Tang et al. 2019), polar waters (Blais et al. 2012; Sipler et al. 2017), and waters overlying and within oxygen-deficient zones (e.g., Bonnet et al. 2013; Dekaezemacker et al. 2013; Jayakumar et al. 2017; Selden et al. 2019). This ideological shift is supported by concurrent investigations of the metabolic requirements and growth controls on recently identified diazotrophic taxa, including non-cyanobacteria diazotrophs (e.g., Zehr et al. 1998; Farnelid et al. 2013) and the haptophyte symbiont cyanobacterium UCYN-A (Zehr et al. 2008; Moisander et al. 2010; Thompson et al. 2012), which differ markedly from those of free-living cyanobacteria such as *Trichodesmium*. Attempts to define the environmental bounds of oceanic N_2 fixation have inevitably led to measurements of exceedingly low rates that approach the detection limits of the $^{15}N_2$ rate measurement methods and that are difficult to reconcile with gene-based metrics of diversity and abundance (*see* Turk-Kubo et al. 2014; Gradoville et al. 2017; Turk-Kubo 2017). This fact has necessarily brought greater attention to the need for routine determination and reporting of lower limits of detection and quantitation. To this end, some inherent analytical and statistical challenges must be examined to enable comparison of rate estimates among researchers, and to extrapolate rate measurements to the regional or global scale.

In this context, we present a critical review of the various $^{15}N_2$ tracer-based protocols currently used to estimate marine N_2 fixation rates. We discuss the advantages and limitations of each, consider the inherent experimental and analytical constraints and assumptions, and examine how these challenges may be addressed in order to provide a roadmap for consistent measurement of pelagic N_2 fixation rates across diverse marine environments. In so doing, we seek to facilitate the comparison and extrapolation of incubation-based rates across the global ocean. Although this review highlights the myriad of issues potentially associated with $^{15}N_2$ tracer incubations, the $^{15}N_2$ tracer assay remains the most sensitive and potentially accurate means of directly estimating N_2 fixation rates. Our aim is thus not to discourage its use, but rather to provide a "best practices" guide for its application in addressing current scientific questions. Ultimately, we hope that this resource will inspire researchers—including new researchers entering the field—to measure water column N_2 fixation and serve as a path forward for better understanding pelagic N_2 fixation and the oceanic N budget.

Stable isotope tracer-based techniques for quantifying N_2 fixation rates

The $^{15}N_2$ fixation method follows the basic steps of any stable-isotope tracer incubations: A water sample is amended with a labeled compound ($^{15}N_2$ gas in this case), incubated under natural or simulated environmental conditions, and the incorporation of the isotopic tracer into a target pool (particulate N) is monitored over time. Rates of N_2 fixation are then calculated from the following equation (Montoya et al. 1996):

$$\text{N}_2\text{ fixation rate (NFR)} = \frac{(A_{\text{PN}} - A_{\text{PN}_0})}{(A_{\text{N}_2} - A_{\text{PN}_0})} \times \frac{[\text{PN}]}{\Delta t} \quad (1)$$

where A_{PN_0} and A_{PN} represent the fractional ^{15}N-enrichment of the particulate nitrogen (PN) pool prior to and following the incubation, respectively, reported in units of atom % (i.e., $^{15}\text{N}/[^{15}\text{N} + ^{14}\text{N}] \times 100$). A_{N_2} is the fractional ^{15}N-enrichment (atom%) of the N_2 source pool, [PN] is the concentration of PN at the end of the incubation period (generally in units nmol N L^{-1}), and Δt is the length of the incubation.

The N isotope ratios of particulate material measured by mass spectrometry are sometimes expressed in delta notation (δ^{15}N) vs. N_2 gas in air, in per mille units:

$$\delta^{15}N(‰) = \left[\frac{^{15}N/^{14}N_{sample}}{^{15}N/^{14}N_{ref}} - 1\right] \times 1000 \quad (2a)$$

Delta values must be converted to atom% values (A_{PN}) in order to compute N_2 fixation rates from Eq. 1. The ^{15}N atom% of particulate material (A_{PN}) can be derived from the $^{15}N/^{14}N$ ratio of the sample (*see* Hayes 2004),

$$^{15}N/^{14}N_{PN} = \left(\frac{\delta^{15}N_{PN}}{1000} + 1\right) \times {}^{15}N/^{14}N_{air} \quad (2b)$$

$$A_{PN}(\%) = \left(\frac{^{15}N/^{14}N_{PN}}{1 + {}^{15}N/^{14}N_{PN}}\right) \times 100 \quad (2c)$$

where the $^{15}N/^{14}N$ ratio of N_2 in air is 0.003676 (Mariotti 1983).

Original method

In the protocol originally described by Montoya et al. (1996), an aliquot of ^{15}N-labeled N_2 gas is injected into incubation bottles with no gaseous headspace. The incubation bottles are sometimes mixed "gently" or inverted to facilitate equilibration of the $^{15}N_2$ gas bubble. Bottles are incubated, typically for 6–24 h (*see* "Additional elements of experimental design" section), then individually filtered through a combusted filter (e.g., glass fiber or silver) to capture particulate material. Incubation volumes and incubation times—from gas injection to filtration—are recorded, and the mass and ^{15}N atom% of particulate N are measured on an elemental analyzer coupled to an isotope ratio mass spectrometer (EA-IRMS). The initial atom% of the dissolved pool, A_{N_2}, is calculated assuming complete isotopic equilibrium of the tracer addition:

$$A_{N_2\,calc} = \frac{([N]_{add} \times A_{add}) + ([N]_{eql} \times A_{eql})}{[N]_{add} + [N]_{eql}} \quad (3)$$

$[N]_{add}$ is the concentration of added $^{15}N_2$ calculated from the ideal gas law ($PV = nRT$) and the sample volume and $[N]_{eql}$ is the N_2 concentration at equilibrium with the atmosphere, derived from gas solubility equations of Weiss (1970) or Hamme and Emerson (2004). A_{add} and A_{eql} represent the ^{15}N atom% of the corresponding N pools. The mole fraction of ^{15}N at natural abundance in dissolved N_2 equilibrated with air, A_{eql}, is 0.3663 atom% (Mariotti 1983). A_{add} is reported by the tracer manufacturer, and is generally around 98–99 atom% $^{15}N_2$.

The original protocol requires minimal manipulation of the water samples. Mohr et al. (2010), however, raised a concern that the equilibration of $^{15}N_2$ gas is relatively slow and ultimately incomplete over the course of most incubations. Reports indicate that the $^{15}N_2$ gas addition equilibrates over a period of ~ 3–15 h, reaching an asymptote at 60–100% of full equilibration, with the degree of equilibration depending largely on the choice of additional mixing steps (Fig. 1; *see* Mohr et al. 2010; Jayakumar et al. 2017; Wannicke et al. 2018). Thus, the fraction of ^{15}N-labeled gas increases from the onset of the incubation, voiding the assumption of constant A_{N_2} (Eq. 1). Incomplete equilibration relative to that predicted based on gas solubility laws can reportedly result in significant underestimation of N_2 fixation rates (Großkopf et al. 2012; Wilson et al. 2012).

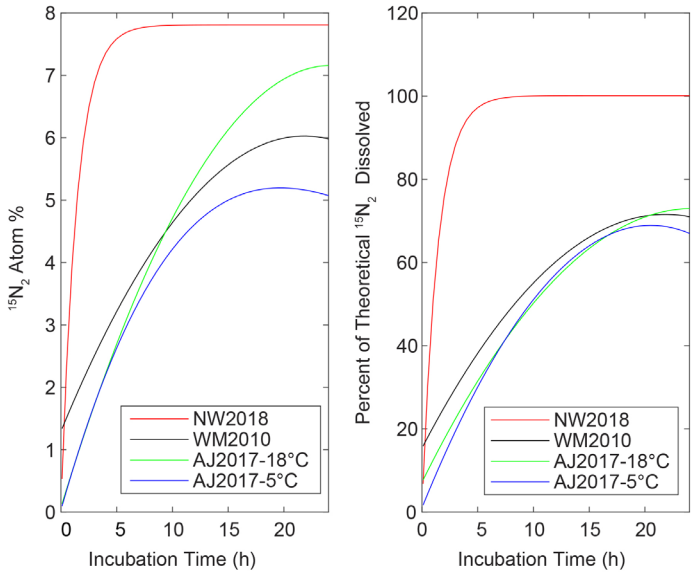

Fig. 1. Range of $^{15}N_2$ gas equilibration curves reported by Wannicke et al. (2018; NW2018), Mohr et al. (2010; WM2010), and Jayakumar et al. (2017) at two incubation temperatures, 18°C and 5°C (AJ2017-18C and AJ2017-5C). Note that in Wannicke et al. (2018), bottles were agitated for 5 min and the incubations were carried out on a horizontal shaker table (10 rpm) to enhance dissolution. Mohr et al. (2010) initially inverted samples 50 times (~ 3 min of agitation). Jayakumar et al. (2017) did not agitate the incubations. All curves are the polynomial fits to the reported measurements.

Dissolution method

Several research groups have proposed modifications to the original protocol to ensure that $^{15}N_2$ concentrations remain constant over the incubation. These protocols also advocate that the $^{15}N_2$ in the incubations should be measured. Mohr et al. (2010) and Klawonn et al. (2015) developed an "enriched seawater technique" (aka, "the dissolution method"), which is similar to that described in Glibert and Bronk (1994). Filtered seawater is enriched with $^{15}N_2$ gas following various protocols designed to encourage gas dissolution (e.g., agitation, cooling, degassing, etc.). This $^{15}N_2$-enriched inoculum is then added to incubations to a target $A_{N_2} \geq 5$ atom%, requiring an inoculum addition on the order of 10% of the total incubation volume. The $^{15}N_2$ in the enriched seawater inoculum can reach concentrations of nearly 90 atom% (e.g., Wilson et al. 2012), whereas the final $^{15}N_2$ atom% of the N_2 source pool in the seawater incubations

(A_{N_2}) is reportedly 2–5% (e.g., Wilson et al. 2012; Gradoville et al. 2017). Importantly, in this method, A_{N_2} remains constant throughout the incubation. The ^{15}N atom% of the dissolved $^{15}N_2$ gas inoculum or of the incubations is verified directly by membrane inlet mass spectrometry (MIMS; *see* Kana et al. 1994) or IRMS ("Methodological considerations for $^{15}N_2$ fixation rate measurements" section).

Of concern in the enriched seawater method is that the preparation of the $^{15}N_2$ inoculum has the potential to modify the incubation matrix substantively. The additional manipulations may result in the introduction of contaminants to the incubations, such as nutrients and/or trace metals, which could artificially stimulate or otherwise diminish diazotroph activity (Klawonn et al. 2015). In this respect, however, we consider that the $^{15}N_2$ tracer gas stock is compressed in a metal tank, dispensed via a metal regulator, and introduced to the incubations with a glass gas-tight syringe with a metal needle—such that trace metal contaminants are likely introduced to incubations regardless of protocol. Nevertheless, preparation of the filtered seawater inoculum requires degassing prior to $^{15}N_2$ gas injection, which removes dissolved gases other than N_2 (e.g., O_2, CO_2), altering seawater pH in addition to ambient gas concentrations. The removal of CO_2 from the seawater inoculum can result in carbonate precipitation, altering alkalinity. Analogous changes in seawater chemistry can also occur when adding the N_2 gas aliquot to the incubations directly, albeit to a lesser extent (*see* Mohr et al. 2010). Despite these limitations, the dissolution method nevertheless offers a means of measuring N_2 fixation that does not violate the fundamental assumption of tracer experiments (however, *see* "Misuse of MIMS to quantify N isotopologue concentrations in the $^{15}N_2$ aliquot." section).

Bubble release method

In order to minimize the inadvertent addition of contaminants to the incubations and moderate changes in incubation pH and alkalinity, the "bubble release technique" has also been employed (aka, "the modified bubble method"; Klawonn et al. 2015; Chang et al. 2019). A $^{15}N_2$ gas aliquot is added to the incubation bottle, mixed gently for ≤ 15 min in order to facilitate $^{15}N_2$ equilibration, and the gas bubble is displaced with unenriched sample water (Klawonn et al. 2015; Chang et al. 2019). Prior to filtration at the end of the incubation period, subsamples are collected to quantify the ^{15}N atom% of the dissolved $^{15}N_2$ gas in each incubation by MIMS or IRMS. As with the enriched seawater technique, the initial atom% of the N_2 source pool (A_{N_2}) is on the order of 2–7 atom% (Chang et al. 2019; White et al. unpubl.), although the level of enrichment reached depends on the quantity of $^{15}N_2$ initially added, the time and type of agitation employed, and on the water temperature. This variant of the method also ensures a uniform proportion of ^{15}N gas tracer throughout the incubation. However, the initial agitation of incubation bottles to promote gas dissolution may stress diazotrophs, as would some applications of the original method (e.g., Wannicke et al. 2018). Furthermore, the simultaneous mixing of individual incubation bottles may require space and personnel. Nevertheless, while more labor-intensive at the onset of the incubation, the bubble release approach minimizes the risk of substantively altering the incubation matrix, while addressing the $^{15}N_2$ gas equilibration concerns discussed above.

Comparison of experimental approaches

While the original $^{15}N_2$ tracer protocol offers the simplest experimental approach to detect N_2 fixation, this method generally underestimates N_2 fixation rates due to the time-dependent and often incomplete equilibration of $^{15}N_2$ gas. Direct comparisons between the original vs. enriched seawater methods have yielded approximately twofold differences in observed N_2 fixation rates (Mohr et al. 2010; Großkopf et al. 2012; Wilson et al. 2012). Wannicke et al. (2018) recently argued, however, that the magnitude of the error is a function of the offset between the time of gas injection and the onset of N_2 fixation. Specifically, they calculated that while N_2 fixation would be underestimated by 72% if it occurred over a short incubation period (1 h), it would be underestimated by only 0.2% for a 24 h incubation, albeit, *if* N_2 fixation began > 6 h following $^{15}N_2$ gas injection and lasted for a 12 h period, following a diel cycle. Otherwise, given a diazotrophic community fixing N_2 at a constant rate from the onset of the incubation for a 24 h period, the N_2 fixation rate would reportedly be underestimated by only 6%. While a 6% uncertainty is acceptable, we note that this error estimate is extrapolated from a significantly more rapid equilibration of $^{15}N_2$ compared to that observed by other research groups (~ 3 h vs. ~ 12 h to asymptote; Fig. 1), likely due to the continuous incubation on a shaker table (Wannicke et al. 2018).

We conducted an analogous sensitivity analysis from a finite-differencing model of N_2 fixation incubations otherwise parameterized for the slower range of $^{15}N_2$ dissolution rates reported (as shown in Fig. 1), and assuming constant N_2 fixation rate over a 24 h period (Supporting Information Section S1). The analysis suggests that N_2 fixation rates can be underestimated by 35–50% by the original method (Supporting Information Fig. S1), concurring with direct comparisons (Mohr et al. 2010; Großkopf et al. 2012; Wilson et al. 2012). Thus, a thorough accounting of the error inherent to the original method across studies requires both an estimation of the equilibration curve resulting from the exact method for bubble injection/mixing used (Fig. 1), as well as an understanding of the timing of biological N_2 fixation in the system of interest. While the former is feasible if the $^{15}N_2$ atom% is monitored throughout an incubation (e.g., Jayakumar et al. 2017), the latter is not. The periodicity (diel variability) of in situ N_2 fixation in mixed, natural diazotroph communities is seldom known a priori, but differs across individual diazotroph groups (Zehr and Turner 2001). Diazotrophs show substantial differences in relative N_2 fixation activity over the day–night cycle, such that variability

of gas enrichment over the incubation period could introduce a taxon-specific bias (Großkopf et al. 2012). For these reasons, the magnitude of the underestimation of the original method may be difficult to ascertain across studies, if not altogether impossible. An alternative strategy that has been used to account for incomplete $^{15}N_2$ dissolution is to correct the calculated rate mathematically for an exponentially averaged enrichment value measured over the incubation period (Jayakumar et al. 2017). However, this method similarly relies on the assumption that N_2 fixation rates are constant over the incubation period, a presumption that is likely not valid in most systems.

In practice, initial A_{N_2} values are similar for both the enriched seawater and the bubble release techniques, typically 2–7 atom%. Additionally, while the target $^{15}N_2$ enrichment in the original technique is generally ~10 atom%, the actual A_{N_2} integrated over the duration of the incubation is usually on the order of ~5 atom% (Jayakumar et al. 2017; Fig. 1), thus comparable to $^{15}N_2$ atom% achieved with the enriched seawater and bubble release techniques. Moreover, A_{N_2} achieved with the enriched seawater and the bubble release techniques may be sufficiently elevated to detect relatively low N_2 fixation rates in most, but not all, aquatic systems. As illustrated in Fig. 2, the minimum detectable N_2 fixation rate decreases with increasing A_{N_2}, while it increases as a function of the particulate nitrogen (PN) concentration in the incubation. The limit of detection (LOD) herein derives from the minimum detectable difference in the ^{15}N enrichment of PN between time initial and time final ($^{min}\Delta A_{PN}$ = 0.00146% or ~4‰) prescribed by Montoya et al. (1996), where N_2 fixation rates are calculated as the minimum detectable $^{min}\Delta A_{PN} \times [PN] \times (A_{N_2})^{-1}$ (Eq. 1, assuming $A_{N_2} - A_{PN_0} \approx A_{N_2}$). Effectively, at an ambient [PN] of 0.3 μmol L^{-1} typical of the oligotrophic ocean, a protocol that achieved $A_{N_2} \geq 3\%$ would hypothetically enable the detection of N_2 fixation rates >0.1 nmol L^{-1} d^{-1}, notwithstanding other sources of uncertainty. This lower A_{N_2} value is thus adequate to detect N_2 fixation in surface waters of subtropical gyres, where biomass is relatively low and rates typically range approximately between 1 and 5 nmol N L^{-1} d^{-1}. Not considered in Fig. 2, however, is whether the prescribed minimum detectable PN ^{15}N change ($^{min}\Delta A_{PN}$) can be resolved by mass spectrometry for incubations at relatively low PN concentrations, a caveat that we discuss in detail further below (*see* "Quantifying the PN pool atom% (A_{PN}) and concentration of PN" section). In any case, at a [PN] of 10 μmol L^{-1}, expected of more productive systems, N_2 fixation rates must exceed 4.9 nmol L^{-1} d^{-1} in order to be detectable given an $A_{N_2} \geq 3\%$, whereas an $A_{N_2} \geq 10\%$ would lower this LOD to 1.5 nmol L^{-1} d^{-1}. The range of $^{15}N_2$ enrichments (A_{N_2}) generally achieved with the enriched seawater and bubble release techniques may thus be insufficient to detect relatively low N_2 fixation rates in more productive ecosystems. This limitation can potentially be overcome by adding a larger aliquot of $^{15}N_2$ to incubations performed using the bubble release technique.

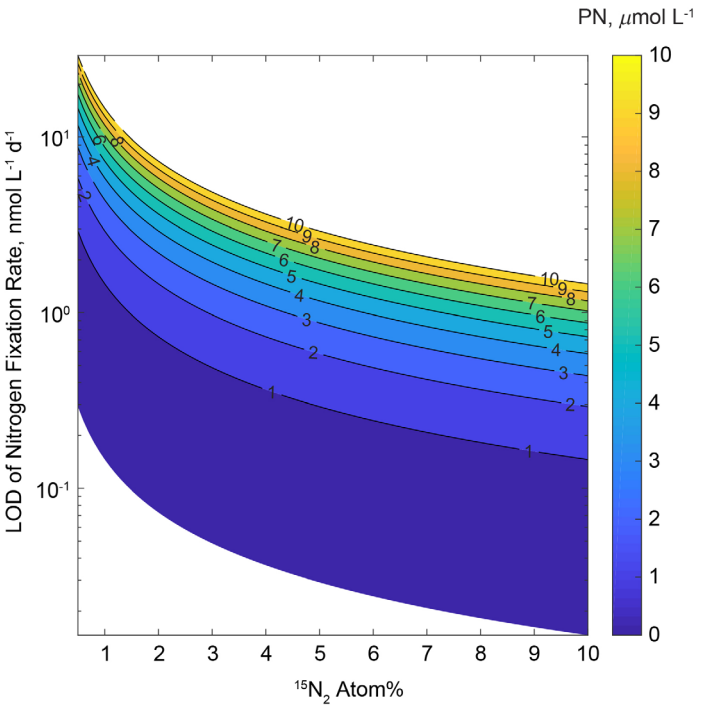

Fig. 2. The hypothetical LOD of N_2 fixation rates in aqueous incubations with $^{15}N_2$ tracer method (y-axis) as a function of the $^{15}N_2$ enrichment (A_{N_2}; x-axis) and the ambient particulate nitrogen concentration ([PN]; colors). The LODs are calculated from Eq. 1 assuming a minimum detectable difference in the ^{15}N enrichment of initial and final PN ($^{min}\Delta A_{PN}$) of 0.00146% (or ~4‰) as per Montoya et al. (1996), where LOD = $^{min}\Delta A_{PN} \times [PN] \times (A_{N_2})^{-1}$.

In all, while the original method requires the least manipulations, rate estimates thus gleaned are subject to uncertainty that is nearly impossible to constrain relative to the uncertainty inherent to the two other method variants. For these reasons, we discourage investigators from resorting to the original protocol. We do not, however, make a recommendation as to which of the other two protocols to follow (enriched seawater vs. bubble release), as there is not yet a sufficient empirical basis from which to ascertain whether one protocol is superior to the other. The enriched seawater method involves greater risk of modifying the incubation matrix, such as the carbonate buffering system, while the initial agitation of the incubations bottles requisite in the bubble release method may be deleterious to more fastidious N_2 fixing organisms, such as *Trichodesmium* colonies. At this junction, it behooves investigators to perform well-controlled intercomparison studies in different systems to assess whether these two protocols yield appreciably different rate estimates. In this regard, we suspect that the variability among incubations replicates may prove greater than that between methodological approaches. Regardless, intercomparison of the protocols remains necessary. More importantly, we believe that intercomparability

among studies and research groups will be realized by adopting robust and standardized analytical protocols and by heeding analytical and experimental uncertainty. We elaborate on these elements in the subsequent sections.

Methodological considerations for $^{15}N_2$ fixation rate measurements

Accurate determination of N_2 fixation rates requires careful quantitation of each variable in Eq. 1. If measured directly, the error associated with each variable must be derived and propagated, and the suitability of any implicit assumptions must be considered within the context of the environment and experiment. Here, we expand upon concerns regarding the determination of source, A_{N_2}, and initial and final particulate atom% values, A_{PN_0} and A_{PN}.

Quantification of the N_2 pool atom% (A_{N_2})

The isotopic composition of dissolved N_2 gas can be quantified by IRMS (e.g., Emerson et al. 1999; Charoenpong et al. 2014). While difficult to quantify accurately at natural abundance (Bender et al. 1994; Emerson et al. 1999), $^{30}N_2$ (^{15}N–^{15}N) is easily detectable in the range of enrichments typical of $^{15}N_2$ fixation incubation experiments. As an example, a serial dilution of 98–99 atom% $^{15}N_2$ gas stock (Cambridge Isotope Laboratories, Lot #I-21065) in air and helium returned the expected signal (i.e., a slope not significantly different from unity) on a continuous flow Delta V Advantage Plus IRMS (Fig. 3a), demonstrating the accuracy of the IRMS over a wide range of $^{15}N_2$ abundances.

Most investigators rely on MIMS to estimate dissolved $^{15}N_2$ gas fractions (*see* N-Fixation Working Group 2019a). Gas measurements of liquid samples require minimal sample manipulations (i.e., no need to introduce a headspace to the samples or otherwise continuously purge the samples), as the membrane inlet is placed directly in contact with the solution and gases are entrained by vacuum or He carrier into the source.

We tested whether the mass-specific signal ratios returned by MIMS accurately quantitate the relative isotopic abundance of $^{15}N_2$ in the range typically used for N_2 fixation incubations. Incremental $^{15}N_2$ gas aliquots were equilibrated in seawater, and respective solutions were then dispensed into replicate gas-tight vials. The ^{15}N atom% values of dissolved N_2 were measured in parallel by continuous flow IRMS on a continuous flow Isoprime IRMS (Charoenpong et al. 2014) and by MIMS (Bay Instruments), on the assumption that values returned by IRMS are accurate (Fig. 3a). The measurements generated on the MIMS were comparable to those by IRMS for the experimental solutions (Fig. 3b). Reassuringly, our MIMS atom% measurements appeared reliable over the broad range of ^{15}N-enrichments (≤ 10 atom%) commonly used in $^{15}N_2$ fixation rate measurements.

Measurements of N isotope abundances of N_2 on the MIMS have hitherto been standardized from a one-point calibration of air-equilibrated seawater at ambient temperature, and extrapolated to the experimental atom% $^{15}N_2$ range (e.g., Böttjer et al. 2017). The MIMS detector, however, is not sufficiently sensitive to resolve $^{30}N_2$ at natural abundance, thus rendering calibrations to air-equilibrated seawater suspect. To clarify this notion, we consider the basic operation of MIMS instruments. In theory, N_2 isotopologues introduced into the source are partially ionized in proportion to their relative abundances, to $^{14}N_2^+$, $^{14}N^{15}N^+$, and $^{15}N_2^+$ ions—corresponding to mass-to-charge ratios (m/z) of 28, 29, and 30. For air-equilibrated water, however, we noted that the ion current recorded by MIMS at m/z 30 is proportionally greater than expected from the natural abundance of $^{30}N_2$ relative to corresponding ion currents for $^{28}N_2$ and $^{29}N_2$ isotopologues.

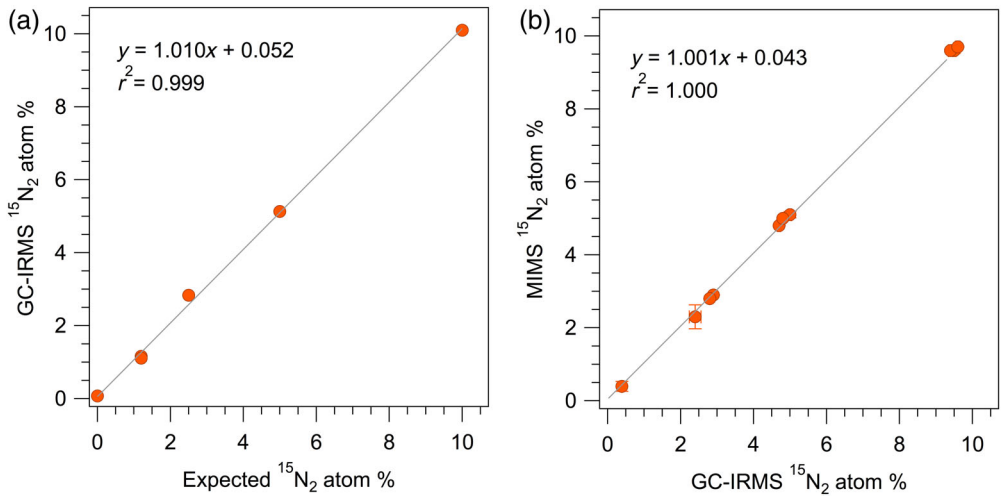

Fig. 3. (**a**) The ^{15}N atom% of N_2 for $^{15}N_2$ gas aliquots in air and helium, measured by continuous flow IRMS (as per Smith et al. 2015). (**b**) The ^{15}N atom% of N_2 dissolved in seawater measured by MIMS (Bay Instruments) vs. by continuous flow IRMS (as per Charoenpong et al. 2014). The ^{15}N atom% of N_2 was calculated as per Eq. 4. Error bars in panel (**b**) are the standard deviations of measurements of triplicate subsamples of dissolved $^{15}N_2$ stocks that were dispensed in parallel into individual 120 mL serum bottles (IRMS) and Exetainer™ vials (MIMS).

Much of the detected signal at m/z 30 at natural abundance may thus originate from instrumental noise and/or interfering ions. Extrapolation of the signal-to-analyte ratio at natural abundance to a tracer-abundance "standard curve" of N_2 isotopologues may therefore yield an erroneous relationship. Conversely, while instrumental noise is sizeable at natural abundance, it is negligible at tracer abundances, such that ion currents should be proportional to the N_2 isotopologue abundances, and thus need not be "calibrated" to air-equilibrated seawater (barring a nonlinear instrumental response—see next paragraph). The parameter A_{N_2} can thus calculated directly from the isotopologue ion currents, as per Eq. 4, where m/z_{28}, m/z_{29}, m/z_{30} denote the respective ion currents:

$$\text{MIMS}\, A_{N_2}\,(\%) = \left[\frac{\frac{m}{z30} + 0.5 * \frac{m}{z29}}{\frac{m}{z28} + \frac{m}{z29} + \frac{m}{z30}}\right] \times 100 \qquad (4)$$

Air-equilibrated seawater at a set temperature should nevertheless be measured periodically throughout sample analysis to monitor signal stability. An example of a spreadsheet for MIMS calculations is provided here (Supporting Information Templates A).

While the ion currents of ionized N_2 isotopologues should theoretically be proportional to their relative concentrations in the samples at tracer abundances (Fig. 3a), both MIMS and IRMS have the potential to respond nonlinearly to N_2 isotopologues in given samples. Care should be taken to account for this effect. Nonlinearity of the response of a given mass spectrometer may be due to several factors. Notably, the extent of isotopic fractionation of N_2 isotopologues during ionization in the source can differ among samples with different gas matrices, skewing isotopologue ratios. This effect, however, will be more pronounced in the atom% range closer to natural abundance, where expectedly slight ionization isotope effects can result in relatively important isotopic offsets (*see* "Quantifying the PN pool atom% (A_{PN}) and concentration of PN" section). Nonlinear responses can also occur at relatively high analyte abundances if the detector becomes saturated. Moreover, interfering ions of similar m/z as N_2 isotopologues can also cause nonlinear responses: In the presence of molecular O_2, N_2 in the source can ionize to NO^+, whose m/z of 30 overlaps with that of ionized $^{15}N_2$ (Jensen et al. 1996; Emerson et al. 1999; Eyre et al. 2002). The measurements presented here were conducted with a MIMS and an IRMS each equipped with high-temperature copper reduction columns to scrub O_2 from the gas stream entering the source (Fig. 3b). However, samples measured in parallel on the IRMS and on the MIMS *without* the O_2 scrubbing column yielded similar ^{15}N atom% values (Supporting Information - Section S2, Fig. S2), indicating that any NO^+ generated in the respective IRMS and MIMS sources was insufficient to alter the ^{15}N atom% significantly in the range pertinent to $^{15}N_2$ tracer incubations.

We caution that individual instruments, instrumental calibrations, filament types, and/or filament ages can result in different linearity responses. To compensate for potential nonlinear responses, standards that match or bracket the gas composition and atom% of the samples should be analyzed concurrently with samples. These standards can be used to quantify the nonlinear response and, if it is significant, to correct the measurements. A method for making dissolved $^{15}N_2$ enriched standard solutions is detailed in Supporting Information Section S3.

Misuse of MIMS to quantify N isotopologue concentrations in the $^{15}N_2$ aliquot

In some variants of the enriched seawater method, the respective *concentrations* of N_2 isotopologues in the $^{15}N_2$-enriched seawater aliquot—rather than their relative abundances—need to be determined, in order to derive A_{N_2} in the incubations into which the inoculum is diluted. N isotopologue concentrations in the $^{15}N_2$-enriched inoculum are extrapolated from their respective ion currents measured by MIMS and normalized to the ion-current-to-concentration of N_2 isotopologues in air-equilibrated seawater (*see* sample calculations in Supporting Information Section S4). However, the ratio of N_2 isotopologue ion currents vs. the respective isotopologue concentrations in enriched seawater is likely *not* proportional to that of air-equilibrated seawater, because the ionization efficiency of gases in the source is influenced by the gas matrix (*see* Sharp 2017): The larger the total sum of gases in the source, the lower the ionization efficiency of respective gases, thus, the lower the respective ion currents recorded by the detector. Because the $^{15}N_2$-enriched inoculum is generally made from degassed seawater, the gas matrix therein is likely to be sufficiently different from that of equilibrated seawater to result in a significantly different ionization efficiency of N_2 isotopologues (and other gases), potentially rendering extrapolation from air-equilibrated seawater incorrect. Such extrapolation will result in inaccurate estimates of the ^{15}N atom% of dissolved N_2 gas in incubations performed with the enriched seawater method.

As a demonstration of the consequences of erroneously presuming that MIMS instruments return measures of absolute gas concentrations, we tested whether MIMS measurements of N_2 gas isotopologues in $^{15}N_2$-enriched inocula yield expected ^{15}N atom% values in the incubations. Our methods are detailed in Supporting Information Section S4, and the corresponding MIMS measurements are provided in Supporting Information Templates A. In all trials, the ^{15}N atom% of dissolved N_2 measured in the incubation bottles was significantly different than that extrapolated from measurements of the $^{15}N_2$-enriched inocula (by –19% to 82%, Table 1). In trials A1–A4, conducted with $^{15}N_2$-enriched inocula prepared by adding $^{15}N_2$ gas to air-equilibrated freshwater followed by vortex mixing (as per Klawonn et al. 2015), measured $^{15}N_2$ atom% values in corresponding incubations were greater than expected. Gas pressures in the source were evidently greater when measuring the inocula than when measuring the

Table 1. The ^{15}N atom% of dissolved N_2 gas in $^{15}N_2$-enriched water inocula and in corresponding incubations (n = 2–3 per inoculum) measured by MIMS (Eq. 4), compared to the expected $^{15}N_2$ atom% in the incubations extrapolated from the atom% of the respective inocula (Supporting Information Section S4). Respective trials A and B were conducted using two different procedures for preparing enriched seawater, described in Supporting Information Section S4.

Trial	$^{15}N_2$ inoculum (atom%)	$^{15}N_2$ measured (atom%)	$^{15}N_2$ extrapolated from air-equilibrated water (atom%)	% Difference vs. expected
A1	35.1 ± 0.2	4.3 ± 0.1	2.4	+82
A2	46.3 ± 0.7	4.7 ± 0.1	3.6	+30
A3	38.5 ± 0.3	2.4 ± 0.0	2.1	+14
A4	41.0 ± 0.2	3.6 ± 0.0	2.7	+34
B1	87.3 ± 0.5	3.0 ± 0.1	3.6	−17
B2	87.3 ± 0.5	2.8 ± 0.1	3.5	−18

air-equilibrated standards, resulting in a proportionally lower ionization of gases from the inocula than from air-equilibrated standards. Consequently, N isotopologue concentrations in the inocula and in the corresponding incubations were underestimated. Conversely, in trials B1–B2, conducted with a $^{15}N_2$-enriched inoculum prepared in vacuum-degassed seawater (Wilson et al. 2012), the measured atom% values in the incubations were lower than expected. The gas pressure in the source was ostensibly lower when measuring the inoculum than air-equilibrated seawater, resulting in overestimated N_2 isotopologue concentrations in the inoculum and in corresponding incubations. These results illustrate that the ^{15}N atom% of dissolved N_2 gas (A_{N_2}) of each incubation bottle should be measured directly (by MIMS or IRMS) rather than extrapolated from that of the $^{15}N_2$-enriched inoculum, as suggested by Klawonn et al. (2015).

Dissolved $^{15}N_2$ sample storage and preservation

MIMS instruments can be installed on board research vessels to measure $^{15}N_2$ atom% directly. In most cases, however, this may prove impractical, in which case $^{15}N_2$ samples need to be stored pending analysis. Investigators typically opt to collect incubation subsamples in Exetainer™ vials, which require advantageously small sample volumes (12 mL), or in crimp-sealed serum bottles, which are anecdotally considered to be more impervious to gas leakage. In this respect, some MIMS instruments consume larger sample volumes to reach a steady signal than accommodated by Exetainer™ vials, in which case sample storage in serum vials is preferable. Dissolved gas samples should be stored without a headspace, as gaseous phase samples are more sensitive to pressure changes and consequent leakage. Gas samples stored in Exetainer™ vials have been shown to lose analyte to the atmosphere on monthly time scales, even under relatively constant storage conditions (Laughlin and Stevens 2003). Aqueous subsamples can be transferred to Exetainer™ or serum vials with gas-tight tubing by gravity or aided by a peristaltic pump. Vials should be overfilled three times, then capped without an air bubble (see technique in Granger 2019). We recommend collecting duplicate or triplicate subsamples, as the inadvertent introduction of small air bubbles will lead to important underestimation of $^{15}N_2$ fractions and, consequently, inaccurate estimation of N_2 fixation rates. Some workers inject concentrated potassium hydroxide, mercuric chloride, or zinc chloride to preserve the samples, although the vials and serum bottles can generally be stored without preservation, as the sum of biological reactions in unpreserved samples during storage is unlikely to generate sufficient N_2 to be of concern, unless working in anoxic waters favoring denitrification (Sturm et al. 2015). Serum bottles and Exetainer™ vials can be stored submerged to curtail direct gas exchange with the atmosphere and minimize potential pressure changes during shipping, a precaution that may be necessary, as discussed below.

We tested the integrity of $^{15}N_2$ gas samples dissolved in seawater samples during storage in Exetainer™ vials, which were kept submerged at 8°C or otherwise left at room temperature unsubmerged. Multiple Exetainer™ subsamples were gravity-filled with discrete 1 L $^{15}N_2$ preparations, and 3–5 Exetainer™ subsamples were measured by MIMS at consecutive time intervals. Statistically significant changes in the ^{15}N atom% of the samples were not evident over a 6-month monitoring period for submerged samples (Fig. 4). Conversely, benchtop samples maintained their integrity for ≤ 40 d, after which $^{15}N_2$ gas decreased detectably. We did not subject any samples to pressure changes from shipping by air freight—such that we cannot assess whether submerging samples is preferable even for shorter-term preservation.

The precision of the dissolved $^{15}N_2$ atom% measured by MIMS averaged 0.1 atom% in our analyses of ≥ triplicate Exetainer™ subsamples (Fig. 4), notwithstanding occasional outliers likely originating from the inadvertent introduction of atmospheric gas bubbles during sample transfer into Exetainers™. This level of uncertainty is negligible at higher $^{15}N_2$ atom% (e.g., 8 atom%), but becomes more important at lower atom% (≤ 2 atom%)—and should be considered if it propagates to a greater uncertainty than the standard deviation

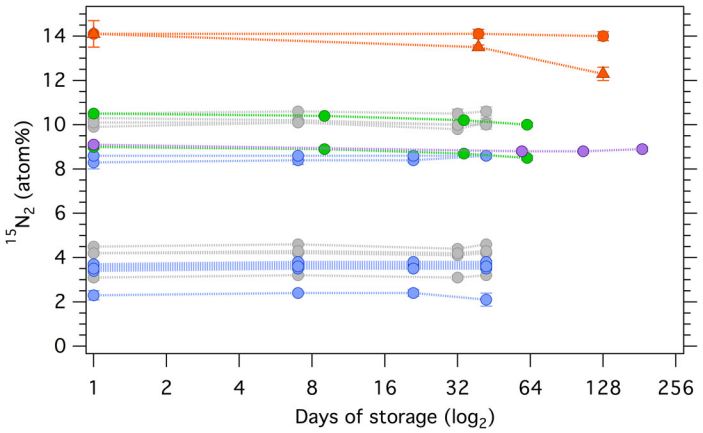

Fig. 4. The fraction of dissolved $^{15}N_2$ gas preserved in Exetainers™ without headspace as a function of storage time, for samples having different initial atom% values. Colors distinguish separate time trials. Circles are subsamples stored submerged at 8°C until analysis, and triangles are subsamples stored at room temperature without being submerged.

among incubation replicates (*see* "Detection limits and error propagation" section).

Quantifying the PN pool atom% (A_{PN}) and concentration of PN

The precision and accuracy of measurements of the initial and final atom% of the particulate material collected on combustible filters are critical determinants of N_2 fixation rates calculated from $^{15}N_2$ incubations. The N isotope ratios ($^{15}N/^{14}N$) of organic material collected from the incubations on silver or glass fiber filters are measured on coupled EA-IRMS instruments. Values are typically reported in $\delta^{15}N$ notation using atmospheric N_2 as the reference (Eq. 2a), and converted to atom% for calculation of N_2 fixation rates (Eqs. 2b, 2c).

The analytical precision of the $\delta^{15}N$ measurement of particulate samples can be relatively high, on the order of 0.2‰ for samples with significant N masses between 40 and 100 μg N. However, measurement precision and accuracy decreases with decreasing sample mass (Fig. 5). The added error can originate from instrumental/atmospheric blanks, N impurities from tin cups and contaminant ions formed due to incomplete combustion or in the source (e.g., CO^+). The accuracy of isotope ratios is also compromised at lower sample masses because the signal becomes progressively nonlinear with decreasing mass due to isotopic fractionation during ionization in the source. The degree of linearity of the instrumental response is a function of the ionization efficiency of gases in the source, which changes with source pressure (Sharp 2017, *see* "Quantification of the N_2 pool atom% (A_{N_2})" section). The extent of isotopic fractionation of isotopologues in the source changes concurrently as a function of the fraction of gas ionized. Linearity is also dependent on factors such as instrument calibration, source configuration, and filament age. In all, isotope measurements at lower N masses are less precise and generally less accurate due to combined effects of multiple factors.

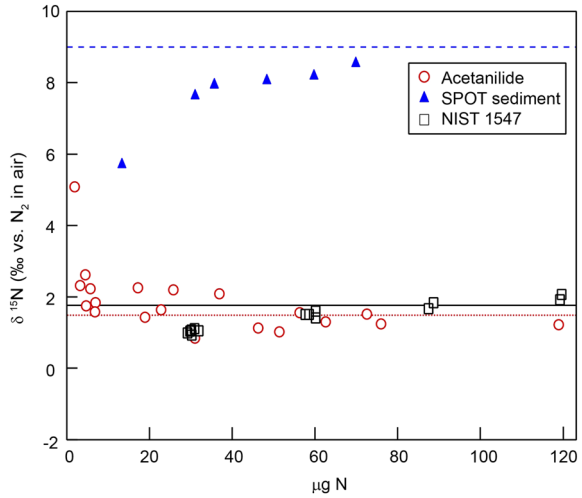

Fig. 5. Examples of the $\delta^{15}N$ measured on EA-IRMS as a function of sample mass, commonly known as "linearity." The acetanilide internal standard with a $\delta^{15}N$ = 1.51‰ (dotted line), compared with acetanilide analyses of variable masses (open circles), NIST 1547 (peach tree leaves) with a $\delta^{15}N$ = 1.95‰ (solid line), compared with NIST 1547 analyses of variable masses (open squares), and San Pedro Ocean Time-series (SPOT) station sediment with a $\delta^{15}N$ = 9.0‰ (dashed line), compared with analyses of variable sediment masses (filled triangles).

Examples of the change in PN $\delta^{15}N$ as a function of sample N mass are shown in Fig. 5 for three different internal N standards, each analyzed on different EA-IRMS systems for masses ranging from 2 to 120 μg N. The mass range over which the measured $\delta^{15}N$ is invariant differs among standards and instruments. In general, $\delta^{15}N$ measurements of samples with < 10 μg N on most IRMS instruments are highly sensitive to sample mass. Our recommendation is thus to collect a minimum of ~ 10 μg of PN per filter if feasible (*see* Fig. 6). Conversely, very high sample N masses or exhausted oxidation EA reactors may also lead to nonlinear and/or apparently enriched $\delta^{15}N$ measurements, due largely to incomplete sample combustion, producing carbon monoxide (CO; Révész et al. 2012). The isotope ratios of CO isotopologues, m/z 29 ($^{13}C^{16}O^+$) to 28 ($^{12}C^{16}O^+$), can be in excess of typical $^{29}N_2/^{28}N_2$ ratios. CO^+ thus "appears" in the analysis as isotopically enriched ^{15}N. In cases of excessive biomass on filters, investigators can split these into replicate samples, but must run both fractions in order to retain information on total concentration PN per volume filtered.

In a parallel vein, we tested whether the addition of ^{13}C-enriched bicarbonate (200 μmol L^{-1} of 99 atom% $H^{13}CO_3^-$; Cambridge Isotope Laboratories) to N_2-fixation incubations—to measure primary production concurrently—can result in m/z 29 enrichment of particulate material due to CO production during combustion, which would mistakenly be interpreted as $^{15}N_2$ incorporation into biomass. We detected no m/z 29 enrichment due to $H^{13}CO_3^-$ addition in 24 h incubations (data not shown), suggesting that incorporation of ^{13}C-label into biomass does not interfere with $^{15}N_2$ incubations—provided the EA reactor is not exhausted.

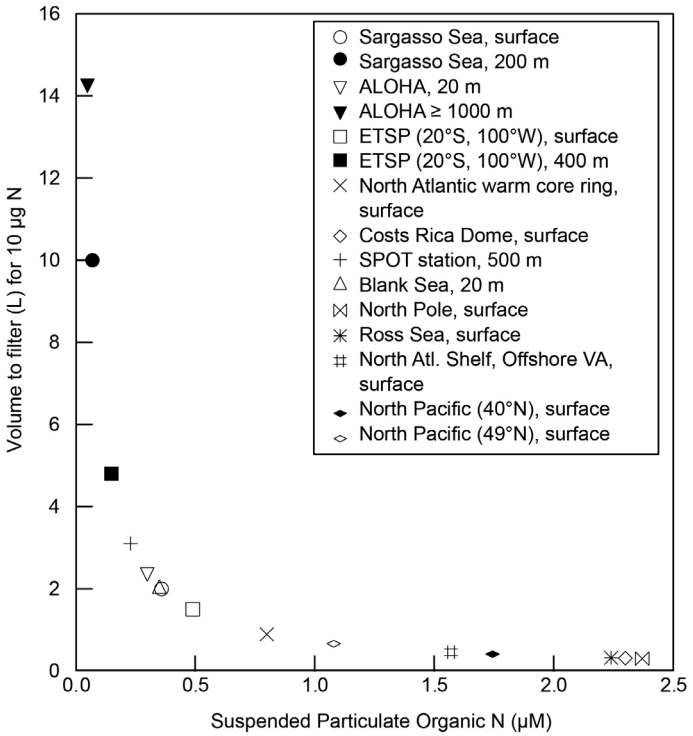

Fig. 6. The sample volume required to yield 10 μg N, a typical minimum detection limit on isotope ratio mass spectrometers. Data source regions are noted in the legend with references as follows: Sargasso Sea (Michaels et al. 1994), Station ALOHA (downloaded from http://hahana.soest.hawaii.edu/hot/hot-dogs/interface.html), the Eastern Tropical South Pacific (Knapp et al. 2016), North Atlantic warm core ring surface waters (Altabet and McCarthy 1985), Costa Rica Dome surface waters (Landry 2014), 500 m at the SPOT station (Hamersley et al. 2011), 20 m in the Black Sea (Coban-Yildiz et al. 2006), surface waters at the North Pole (Matrai and Orellana 2012), surface waters of the Ross Sea (Dunbar 2016), North Atlantic surface waters offshore of Virginia (Oczkowski et al. 2016), and North Pacific surface waters from 40°N and 49°N (A. White unpubl.).

When PN samples are sent to commercial laboratories for $\delta^{15}N$ analysis, internal isotopic reference materials should be included with the sample set to ensure isotopic calibration at the low mass range typical of open ocean incubation conditions. This is particularly important if samples that are below the 10 μg N threshold are considered (*see* "Detection limits and error propagation" section). Accompanying reference materials must be of mass similar to the N mass of the filter samples. As a general practice for all EA-IRMS analyses, replicates of two reference materials whose ^{15}N isotopic compositions bracket the expected PN enrichments should be included with each batch of PN filters for EA-IRMS analysis (Révész et al. 2012). Two-point normalization corrections using the results from the reference materials can then be used to improve the accuracy of the measured PN enrichments in the given mass range. This approach can correct PN data for the combined blank, contamination, and linearity effects. The National Institute for Standard Technology (NIST) website provides a list of isotopic reference materials available, including the widely used USGS 40 and 41 glutamic acids whose C : N is similar to marine organic matter. Finally, we urge investigators who remain intent on carrying out EA-IRMS analyses of low N mass samples to consult and Merritt and Hayes (1994) and Montoya (2008) for more detailed examinations of instrumental and analytical detection limits and reproducibility.

Collecting a sample with adequate mass is straightforward when one has a reasonable estimate of the PN concentration in a given ecosystem (Figs. 6, 7). However, this may pose a challenge when conducting $^{15}N_2$ fixation incubations of oligotrophic, low biomass waters or of mesopelagic waters. Water budgets at sea may be limited, thus reducing the water volumes available for incubations and the quantity of material available for isotopic analysis. Nevertheless, the following practices may help to optimize sample collection for $^{15}N_2$ incubations for isotopic analysis. First, before measuring $^{15}N_2$ fixation at sea, it is recommended that investigators know the lower LOD/quantitation for PN $\delta^{15}N$ analysis for their relevant mass spectrometer. The necessary incubation volume to exceed analytical detection limits can then be estimated from published reports of the range of PN concentrations ([PN]) in the study region and at the water column depths of interest (Figs. 6, 7). For example, if one wanted to measure rates of $^{15}N_2$ uptake at 1000 m in the North Pacific Subtropical gyre, one could estimate [PN] from measurements at Station ALOHA, which are typically ≤ 0.05 μmol L^{-1}, corresponding to ~ 14 L incubation volume to yield 10 μg N (Fig. 6).

Choice of particle filter

The choice of filter onto which to collect PN may also influence the magnitude of N_2 fixation rate estimates. Until recently, Whatman™ GF/F glass fiber filters were routinely used. These have a nominal pore size is 0.7 μm prior to combustion, although filters are reportedly compacted by combustion (to an effective pore size of ~ 0.3 μm), resulting in greater retention of particles (Nayar and Chou 2003). Nevertheless, the retention efficiency of GF/F filters is unclear and has been questioned, specifically for measurements of phytoplankton pigments. Some researchers have reported that GF/F filters perform as well in retaining phytoplankton as 0.2 μm pore-size membrane filters (Li et al. 1983; Yentsch 1983; Goldman and Dennett 1985; Li 1986; Taguchi and Laws 1988; Chavez et al. 1995; Ferrari and Tassan 1996), whereas others have found 0.2 μm membrane filters to be superior (Phinney and Yentsch 1985; Dickson and Wheeler 1993, 1995). An alternate variety of glass fiber filter has recently become available, the Advantec GF-75, which claims a nominal pore size of 0.3 μm. Bombar et al. (2018) demonstrated that nonpigmented particles (bacterioplankton) were more abundant in the filtrate of GF/Fs vs. GF-75, suggesting greater retention of particle mass by the smaller pore-size GF-75. N_2 fixation rates were more likely to be detected in their study regime with GF-75 than GF/F filters, and detected rates were systematically higher with GF-75 filters. Nevertheless, while more retentive than GF/F filters,

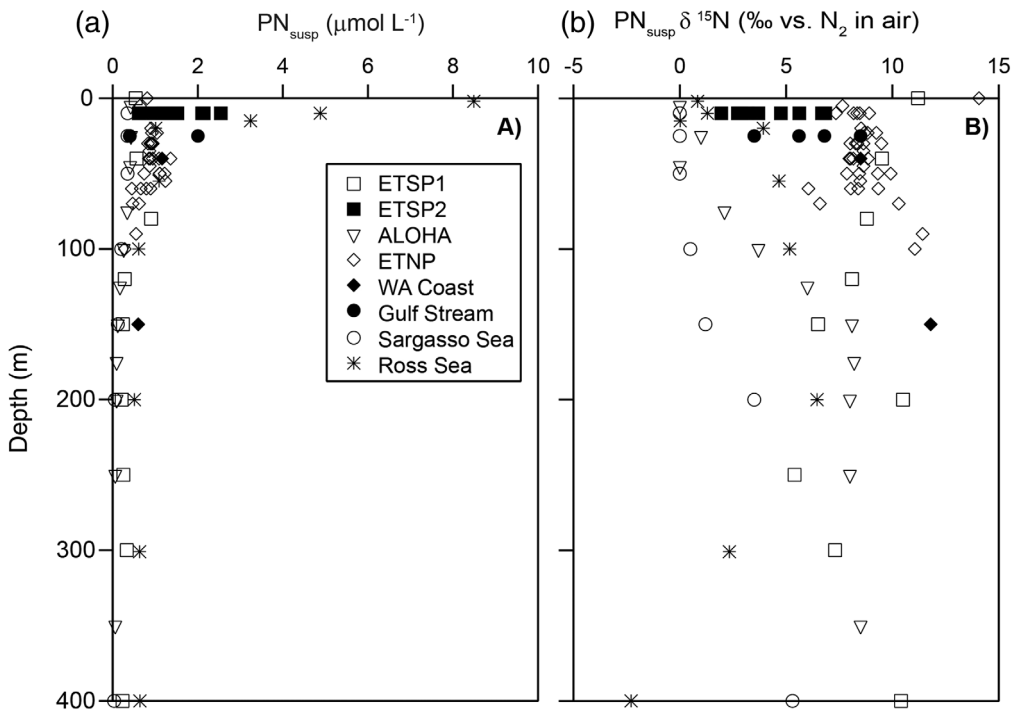

Fig. 7. Range of observed suspended particulate nitrogen (PN) concentrations (**a**) and $\delta^{15}N$ (**b**) in samples collected in the Eastern Tropical South Pacific (Knapp et al. 2016; Gradoville et al. 2017), Station ALOHA (Hannides et al. 2013), the Eastern Tropical North Pacific (White et al. 2013), offshore of Washington state (Gradoville et al. 2017), the Gulf stream (White, unpubl.), the Sargasso Sea (Altabet 1988), and the Ross Sea (Dunbar 2016).

~ 40% of bacterioplankton cells were still lost to the filtrate with GF-75 filters. Moreover, the diazotrophic communities tended to differ markedly between bulk water and filtrates, suggesting differential retention of N_2-fixing communities (Bombar et al. 2018). Similarly, Chaves et al. (IOCCG Protocol Series 2019) reported a small but significant positive mean bias for particulate organic carbon (POC) measured on GF-75 vs. GF/F in small-volume sampling off the Peruvian coast where POC was between 10 and 30 μmol L^{-1}.

To ensure the capture of smaller particles, researchers have otherwise used combusted 0.2 μm pore-size silver filters (e.g., Anapore®), which have relatively slow filtration rates. Chang et al. (2019) observed no difference in the biomass captured by GF/F vs. silver filters at PN concentrations ≤ 1.5 μmol L^{-1}, whereas more PN was captured on GF/F filters at concentrations ≥ 1.5 μmol L^{-1}. The authors attributed this discrepancy to the adsorption of dissolved organic material (DOM) onto GF/F filters: DOM has been shown to adsorb onto glass fiber filters, in proportion to the volume of water filtered (Morán et al. 1999; Turnewitsch et al. 2007; Novak et al. 2018), contributing additional uncertainty to PN concentrations thus estimated. While the resulting N_2 fixation rates observed by Chang et al. (2019) were not coherently related to filter type, there were more instances of rates above the LOD with silver filters.

In all, a clear recommendation on filter choice does not emerge from the sum of published (and anecdotal) evidence. Recognizing that respective filter types have distinct attributes and limitations, we further consider that filtration rates, the volume of seawater filtered, the amount biomass filtered, and the length of the filtration period may exert even greater influence on biomass retention than filter type. We thus remain agnostic as to the choice of filter, but recommend that this variable be clearly identified to inform comparison among studies. We stress that [PN] estimates may be uncertain regardless of filter type, contributing proportionally—yet unaccountably—to uncertainty in the rate estimates.

Considerations on the initial PN $\delta^{15}N$ and on control incubations

N_2 fixation rates are calculated from the change in the $\delta^{15}N$ of the suspended particulate N (PN) over the duration of the incubation. Measurements of the initial PN $\delta^{15}N$ are thus critical to reliably estimate N_2 fixation rates (Eq. 1). Because the $\delta^{15}N$ of PN in the surface ocean of the tropical and subtropical North Atlantic is often, although not always, close to 0‰ vs. air (Fig. 7), some investigators forego collecting initial or "time zero" PN samples, and otherwise rely on the assumption of a 0‰ initial PN $\delta^{15}N$. However, it is not uncommon for the $\delta^{15}N$ of PN to be ≥ 0‰ and upwards of 10‰ in some regions, such as the South Pacific, the western Arctic, continental shelves, and oxygen deficient margins (Fig. 7). An incorrectly assumed initial PN $\delta^{15}N$ can significantly affect the magnitude of N_2 fixation rates. For example, given a PN concentration of 3 μmol N L^{-1}, and assuming a 0‰ initial PN instead of an actual 10‰ initial PN, would result in a presumed change in PN $\delta^{15}N$ of ~ 10‰ (i.e., ΔA_{PN} = 0.0057%) given a A_{N_2} of

5 atom%. This would result in a misdiagnosed N_2 fixation rate of ~ 3 nmol L^{-1} d^{-1}. Thus, the initial $\delta^{15}N$ of PN should always be measured.

The derivation of N_2 fixation rates further relies on the assumption that any change in the ^{15}N atom% of the suspended particulate N (PN) over the incubation period is due to the uptake of the added $^{15}N_2$. To verify this notion, investigators may consider conducting parallel incubations without $^{15}N_2$ to account for naturally occurring changes in the atom% of PN. The $\delta^{15}N$ of PN can change considerably during a 24 h incubation due to the uptake of ambient ammonium, nitrate, or organic nitrogen. Such N uptake is apt to occur in waters incubated from most ocean systems, except perhaps waters from the oligotrophic surface ocean where nutrients are depleted. Inherent changes in $\delta^{15}N$ of PN are of particular concern in incubations supplemented with organic substrates, as growing microbes will assimilate ambient nitrogen (nitrate, ammonium, or organic nitrogen) to exploit newly available carbon substrates, resulting in changes in the atom% of suspended biomass. Moreover, in nearshore regions, where N_2 fixation rates may be low against a background of other N cycling processes, the assimilation of nutrients and N substrates by plankton is likely to overprint any $^{15}N_2$ uptake from coincident N_2 fixation. Without precautionary unenriched control incubations, $^{15}N_2$ fixation rate estimates may yield biased results.

Potential sources of experimental error

When $^{15}N_2$ gas is injected directly into samples, care must be taken to inject a known volume at atmospheric pressure. To this end, the pressure inside the syringe can be equilibrated to atmospheric pressure by opening the valve briefly while the needle tip is submerged in a small beaker filled with water to observe the release of overpressure. This procedure assures that the N_2 is injected into the bottle is not over-pressurized.

Trace-levels of ^{15}N-labeled contaminants have been detected in some commercially available $^{15}N_2$ stocks, which can lead to false positives (Dabundo et al. 2014). The industrial production of $^{15}N_2$ gas generally involves the oxidation of ^{15}N-ammonium to $^{15}N_2$, followed by acid and cryogenic removal of ammonium and other potential nitrogen oxide (NO_x) contaminants. Dabundo et al. (2014) reported that most suppliers provide $^{15}N_2$ stocks remarkably free of ^{15}N impurities, with the exception some Sigma-Aldrich stocks that contained influential levels of ^{15}N-labeled NO_x (as nitrate and/or nitrite) and ammonium. It remains unclear whether this problem has always existed or resulted from a procedural error. Stocks prior to 2010 were not associated with unusually elevated rate estimates (Böttjer et al. 2017), supporting the latter scenario. Regardless, verifying the relative purity of stocks prior to use remains advisable, although this measurement can be impractical and costly as it requires specific methodology (*see* Dabundo et al. 2014). We have thus created a forum from which to disseminate estimates of potential contamination by ^{15}N ammonium and/or ^{15}N NO_x of specific $^{15}N_2$ batches from respective suppliers (*see* N-Fixation Working Group 2019b). Therein, investigators are encouraged to provide metadata on analytical protocols used to generate the measurements. The provenance of these measurements can then be cited in publications. Alternatively, potential contamination can be verified by growing nondiazotrophic microbial cultures in low N media (ca. 100 μmol L^{-1} NH_4^+ or NO_3^-) equilibrated with $^{15}N_2$, to compare the resulting ^{15}N atom% of stationary-phase cells (measured with an EA-IRMS) with those in control cultures (Dabundo et al. 2014).

Best practices for any type of biological incubation mandate the use of acid-washed plastic-ware, rather than glassware. Metal oxides are known to adsorb onto and leach from borosilicate glass (e.g., Struempler 1973), such that biological activity can be either depressed or stimulated from trace-metal contamination. We stress, nevertheless, that carrying out manipulations in acid-washed plastic-ware does not afford the incubations so-called "trace-metal-clean" status, given that $^{15}N_2$ gas stocks are pressurized in metal cylinders—as pointed out earlier. Nevertheless, investigators should still attempt to minimize trace metal contamination by adhering best practices for field incubations, and consider measuring metal concentrations when feasible.

Finally, certain types of laboratory gloves, in particular latex and nitrile gloves, can introduce N contaminants during both water-sampling and filter-handling stages (Makela et al. 1997; Garçon et al. 2017). Use of equipment that has encountered other ^{15}N-containing compounds is similarly problematic. Having ^{15}N-DIN compounds near $^{15}N_2$ tracer assays carries a high chance of cross-contamination and might lead to false positives of N_2 fixation activity. Sharing equipment between N_2 fixation samples and other ^{15}N-substrate assays should be avoided.

Additional elements of experimental design

Given that different diazotrophs fix N_2 over different portions of the light/dark cycle, extrapolation of rates measured over the course of a few hours to an entire day may be misleading. Similarly, a rate estimate based on a 24 h incubation cannot simply be divided by 24 for an accurate hourly rate. Hourly and daily rates should therefore be reported as such and any conversion should be clearly stated to avoid confusion. Similarly, attention must be paid to the units in which N_2 fixation rates are reported, in particular whether rates are in moles of N per volume or moles of N_2 per volume. In the interest of standardizing practices, we recommend 24 h incubations whenever possible and reporting units of nmol N L^{-1} d^{-1} to facilitate comparison of rates across studies and ocean basins.

While incubations should ideally be maintained under in situ light and temperature to avoid stimulation or inhibition of N_2 fixation, in practice, the ability to maintain such conditions is often limited by the available infrastructure and cruise plans. If ambient conditions cannot be approximated, it is critical that the temperature and light levels achieved be reported. Sampling in direct sunlight may lead to

photoinhibition of metabolic processes (Platt et al. 1981) and should therefore be avoided. While sampling and initiation of incubations prior to dawn (in the dark) is preferable, it too may not be logistically feasible, in which case we recommend taking measures to protect samples from direct sunlight during sampling.

Detection limits and error propagation

Several recent studies have reported low N_2 fixation rates (< 1 nmol N L^{-1} d^{-1}) in mesopelagic waters (e.g., Fernandez et al. 2011; Dekaezemacker et al. 2013; Rahav et al. 2013; Benavides et al. 2016). If depth-integrated over the vast expanse of the deep ocean, these low rates are proposed to have a significant impact on the global N budget. Low but potentially important rates highlight the need for standard reporting of accurate detection limits for N_2 fixation measurements. Yet, detection limits are not commonly reported in N_2 fixation studies, and studies which do report detection limits use diverse methods to calculate these.

A number of approaches have been suggested for calculating detection limits associated with the $^{15}N_2$ technique (e.g., Montoya et al. 1996; Gradoville et al. 2017; Jayakumar et al. 2017). Analytically, detection limits are typically defined as an instrument blank plus three standard deviations (MacDougall and Crummett 1980). The original $^{15}N_2$ method described by Montoya et al. (1996) and Montoya (2008) and proposed a LOD for the method that derives from the instrumental detection limit, namely, the minimal detectable difference in the ^{15}N atom% of PN that can be resolved by the EA-IRMS given a sample PN mass of ~ 14 μg ($^{\min}\Delta A_{PN}$). The method LOD is then calculated as (Eq. 5):

$$\mathrm{LOD} = \frac{^{\min}\Delta A_{PN}}{(A_{N_2} - A_{PN_0})} \times \frac{[\bar{PN}]}{\Delta t} \quad (5)$$

Jayakumar et al. (2017) otherwise calculated $^{\min}\Delta A_{PN}$ as three times the standard deviation of seven measurements of a low-mass isotopic standard (Ripp 1996), yielding a $^{\min}\Delta A_{PN}$ of 0.0025 atom% (approximately 7‰) for 12 μg N standards. For the same A_{N_2} values used above, this would indicate a method LOD of 0.2 nmol L^{-1} d^{-1} with a [PN] of 0.3 μmol N L^{-1} and of 0.6 nmol L^{-1} d^{-1} with a [PN] of 1.0 μmol N L^{-1}. Such LOD estimates will vary depending on the environment and corresponding [PN], the precision of the mass spectrometer in the sample PN mass range, and the $^{15}N_2$ enrichments achieved. Importantly, a generic $^{\min}\Delta A_{PN}$ of 0.00146 atom% is not adequate to capture the analytical uncertainty inherent to isotopic measurements of PN masses < 10 μg. Investigators should quantify this uncertainty specifically from measurements of correspondingly low-mass isotopic standards (e.g., Jayakumar et al. 2017). For instance, given a meager PN mass of 2 μg collected on filters, the measurements presented in Fig. 5 suggest a standard deviation of ~ 3‰ for the given mass spectrometer and standard (acetonitrile), which would translate to an *analytical* LOD of 9‰ (0.00330 atom%)—namely, $^{\min}\Delta A_{PN}$ would need to exceed 9‰ in order to claim the detection of an analytically significant ^{15}N-enrichment between the initial and final incubation time points. With a [PN] of ~ 0.3 μmol N L^{-1}, and a 4 atom% A_{N_2}, the *method* LOD would then be 0.3 nmol L^{-1} d^{-1}.

Alternatively, the LOD can be equated to the propagated experimental uncertainty associated with each parameter measurement, as described by Montoya et al. (1996; e.g., Bevington 1969; Gradoville et al. 2017). This LOD variant is calculated as the square root of the sum of the squares of the partial derivative of the N_2 fixation rate (NFR) with respect to the standard deviation (σ) of each of the experimental parameter featured in Eq. 6:

$$\mathrm{LOD} = \sqrt{\left(\sigma_{\Delta t} \times \frac{\partial \mathrm{NFR}}{\partial \Delta t}\right)^2 + \left(\sigma_{A_{N_2}} \times \frac{\partial \mathrm{NFR}}{\partial A_{N_2}}\right)^2 + \left(\sigma_{A_{PN_0}} \times \frac{\partial \mathrm{NFR}}{\partial A_{PN_0}}\right)^2 + \left(\sigma_{A_{PN}} \times \frac{\partial \mathrm{NFR}}{\partial A_{PN}}\right)^2 + \left(\sigma_{[\bar{PN}]} \times \frac{\partial \mathrm{NFR}}{\partial [\bar{PN}]}\right)^2} \quad (6)$$

All parameter names are as described for Eq. 1 and the suggested value of $^{\min}\Delta A_{PN}$ is 0.00146 atom% (approximately 4‰), as per Montoya et al. (1996) and Montoya (2008). Thus, for a 24 h incubation in an oligotrophic region with a [PN] of ~ 0.3 μmol N L^{-1}, and a 4 atom% enrichment of A_{N_2} over ambient PN, the method LOD as per Eq. 5 would be 0.1 nmol L^{-1} d^{-1}—provided sufficient PN mass (≥ 10 μg) was collected on the filter. The method LOD would increase to 0.4 nmol L^{-1} d^{-1} for a [PN] of 1.0 μmol N L^{-1}.

An advantage of using this LOD (Eq. 6) is that these calculations parse the total uncertainty into that associated with each measured parameter. For example, variability in A_{PN_0} may dominate the error in samples with low or undetectable N_2 fixation rates, whereas variability in [PN] may contribute the largest source of uncertainty in samples with high N_2 fixation rates (Montoya et al. 1996; Gradoville et al. 2017).

There are several important considerations for calculations of both LOD variants. First, discrete LODs should be calculated

for individual rate measurements because the calculations depend on parameter values and levels of uncertainty that differ between sets of incubations (Eqs. 5, 6). It is also essential to use the measured [PN] values—and standard deviations of incubation replicates (Eq. 6)—and *not* the minimum [PN] detectable on the mass spectrometer, as the latter would artificially decrease detection limits. Moreover, measurements below the *analytical* (i.e., instrumental) limits of detection should not be considered in computations of the N_2 fixation rate LODs (e.g., EA-IRMS measurements with relatively low PN masses not bracketed by concomitant standard analyses). As stated earlier, A_{PN_0} should be measured explicitly for each depth-specific incubation experiment, in replicate, in order to assess the uncertainty of the measurement to derive the LOD as per Eq. 6. Additionally, the value of A_{N_2} is likely to vary among individual incubation bottles, such that the mean value of A_{N_2} and its standard deviation among incubation replicates (measured directly by IRMS or MIMS; "Quantification of the N_2 pool atom% (A_{N_2})" section) both need to be considered to calculate the LOD as per Eq. 6. Finally, investigators are encouraged to report all N_2 fixation rate estimates, clearly denoting those below the *method* LODs, as the latter provide valuable information about environments in which N_2 fixation is not detected.

We have created templates for calculations of nitrogen fixation rates and associated LODs (*see* "spreadsheet": N-Fixation Working Group 2019c; Supporting Information Templates B). We encourage investigators to use these templates both for calculations and to provide metadata and ancillary data pertinent to the rate calculations in peer-reviewed publications, either as supplementary material or through an accession number within the publicly available OCB N_2 fixation rate database (*see* N-Fixation Working Group 2019a). Standardization of detection limit calculations and the publication of raw data used to calculate N_2 fixation rates will set a precedent of transparency and foster progress towards understanding the patterns and controls of oceanic N_2 fixation.

Summary of recommendations

In opting for a protocol to measure pelagic N_2 fixation rates, we discourage investigators from following the original $^{15}N_2$ tracer method, given its propensity to yield underestimate rates. We otherwise advise employing either the dissolution or bubble release method, whichever is best suited to the specific research objectives and logistical constraints. This latter recommendation may change in time, as more insights on the merits and shortcomings of respective protocols emerge.

The more important aspect of our review involves the critical evaluation of pertinent analytical protocols and experimental designs, based on which we tender guidelines to which investigator should adhere in order to assure confidence in the validity of rate estimates, and to foster intercomparability. Some key points emerge from our analysis, which we reiterate here.

- The $^{15}N_2$ atom% should always be measured directly for each incubation bottle. This value should not be inferred or derived from that of an inoculum, as such extrapolations can lead to substantial error in A_{N_2} and, consequently, in the estimated rates ("Misuse of MIMS to quantify N isotopologue concentrations in the $^{15}N_2$ aliquot." section and Table 1).
- The natural abundance of $\delta^{15}N$ in the PN pool should be measured at time 0, as this value is not uniform among environments or depth ranges ("Considerations on the initial PN $\delta^{15}N$ and on control incubations" section and Fig. 7).
- Control incubations are necessary in environments where the assimilation of ambient DIN can effect potential changes in the PN atom% during the incubations ("Considerations on the initial PN $\delta^{15}N$ and on control incubations" section).
- When possible, incubations should be initiated prior to dawn and incubated for 24 h to account for diel cycles in the rates. Regardless, incubation periods should always be reported and authors should avoid scaling rates measured over periods of less than a day upward to daily units ("Additional elements of experimental design" section).
- Dissolved $^{15}N_2$ gas samples should be stored without a headspace, in Exetainers™ or in serum vials. Exetainer samples preserved submerged maintain their integrity for a longer period of time.
- The purity of commercial $^{15}N_2$ stocks with respect to reactive N contaminants must be verified. Investigators can report on the purity of respective brands and associated batch numbers (*at* N-Fixation Working Group 2019b).
- A minimum of ~ 10 μg of PN per filter ensures adequate sample mass to resolve small differences in N isotope ratios ("Quantifying the PN pool atom% (A_{PN}) and concentration of PN" section, Fig. 5).
- The analytical uncertainty associated with EA-IRMS measurements of lower-mass samples (< 10 μg) must be quantified from measurements of standards at corresponding masses, from which to estimate method LODs ("Quantifying the PN pool atom% (A_{PN}) and concentration of PN" and "Detection limits and error propagation" sections).
- We urge investigators to report the incubation-specific LODs in all publications, to foster transparency and enable cross-comparison among research groups and environments ("Detection limits and error propagation" section).

Finally, in recognizing that N_2 fixation rate estimates are subject to uncertainty that may not be ultimately quantifiable, the occurrence of N_2 fixation and the magnitude of its flux can also be investigated by complementary means and methods, some of which are briefly reviewed here (Supporting Information Section S5)—to arrive at a more comprehensive view.

Conclusions

Biological N_2 fixation is the predominant source of N to the global ocean. As such, N_2 fixation has a rich history of

scientific inquiry that continues to evolve. Here we have surveyed the divergent methodological approaches to the $^{15}N_2$ tracer method to measure N_2 fixation rates in pelagic systems, and provided specific recommendations to standardize and ameliorate aspects of the method, including templates to calculate rates and from which to assess detection limits. While the research community may remain divided as to which variant of the method to follow, the standardization of some key practices will enable intercomparability among estimates, to better discern temporal and biogeographical trends, as well as environmental controls on ocean N_2 fixation. It then behooves researchers to carefully acknowledge and evaluate all potential sources of uncertainty regardless of approach. We have herein provided guidelines to this end. We hope for consideration of these practical recommendations, so that we, as a community, can develop a more robust understanding of the magnitude, variability, and controls on the N_2 fixation in the global ocean.

References

Altabet, M. A. 1988. Variations in nitrogen isotopic composition between sinking and suspended particles - implications for nitrogen cycling and particle transformation in the open ocean. Deep-Sea Res. A **35**: 535–554. doi:10.1016/0198-0149(88)90130-6

Altabet, M. A., and J. J. McCarthy. 1985. Temporal and spatial variations in the natural abundance of ^{15}N in PON from a warm-core ring. Deep-Sea Res. A **32**: 755–772. doi:10.1016/0198-0149(85)90113-X

Benavides, M., P. H. Moisander, H. Berthelot, T. Dittmar, O. Grosso, and S. Bonnet. 2015. Mesopelagic N_2 fixation related to organic matter composition in the Solomon and Bismarck Seas (Southwest Pacific). PLoS One **10**: e0143775. doi:10.1371/journal.pone.0143775

Benavides, M., and others. 2016. Basin-wide N_2 fixation in the deep waters of the Mediterranean Sea. Global Biogeochem. Cycles **30**: 952–961. doi:10.1002/2015GB005326

Bender, M. L., P. P. Tans, J. T. Ellis, J. Orchardo, and K. Habfast. 1994. A high precision isotope ratio mass spectrometry method for measuring the O_2:N_2 ratio of air. Geochim. Cosmochim. Acta **58**: 4751–4758. doi:10.1016/0016-7037(94)90205-4

Bevington, P. R. 1969. Data reduction and error analysis for the physical sciences. McGraw-Hill.

Blais, M., J. É. Tremblay, A. D. Jungblut, J. Gagnon, J. Martin, M. Thaler, and C. Lovejoy. 2012. Nitrogen fixation and identification of potential diazotrophs in the Canadian Arctic. Global Biogeochem. Cycles **26**: GB3022. doi:10.1029/2011GB004096

Bombar, D., R. W. Paerl, R. Anderson, and L. Riemann. 2018. Filtration via conventional glass fiber filters in $^{15}N_2$ tracer assays fails to capture all nitrogen-fixing prokaryotes. Front. Mar. Sci. **5**: 6. doi:10.3389/fmars.2018.00006

Bonnet, S., I. C. Biegala, P. Dutrieux, L. O. Slemons, and D. G. Capone. 2009. Nitrogen fixation in the western equatorial Pacific: Rates, diazotrophic cyanobacterial size class distribution, and biogeochemical significance. Global Biogeochem. Cycles **23**: GB3012. doi:10.1029/2008GB003439

Bonnet, S., J. Dekaezemacker, K. Turk-Kubo, T. Moutin, R. M. Hamersley, O. Grosso, J. P. Zehr, and D. G. Capone. 2013. Aphotic N_2 fixation in the eastern tropical South Pacific Ocean. PLoS One **8**: e81265. doi:10.1371/journal.pone.0081265

Böttjer, D., J. E. Dore, D. M. Karl, R. M. Letelier, C. Mahaffey, S. T. Wilson, J. Zehr, and M. J. Church. 2017. Temporal variability of nitrogen fixation and particulate nitrogen export at Station ALOHA. Limnol. Oceanogr. **62**: 200–216. doi:10.1002/lno.10386

Capone, D. G., and E. J. Carpenter. 1982. Nitrogen fixation in the marine environment. Science **217**: 1140–1142. doi:10.1126/science.217.4565.1140

Chang, B. X., A. Jayakumar, B. Widner, P. Bernhardt, M. R. Mulholland, and B. B. Ward. 2019. Low rates of dinitrogen fixation in the eastern tropical South Pacific. Limnol. Oceanogr. **64**: 1913–1923. doi:10.1002/lno.11159

Charoenpong, C. N., L. A. Bristow, and M. A. Altabet. 2014. A continuous flow isotope ratio mass spectrometry method for high precision determination of dissolved gas ratios and isotopic composition. Limnol. Oceanogr. Methods **12**: 323–337. doi:10.4319/lom.2014.12.323

Chavez, F. P., K. R. Buck, R. R. Bidigare, D. M. Karl, D. Hebel, M. Latasa, and L. Campbell. 1995. On the Chlorophyll *a* retention properties of glass-fiber GF/F filters. Limnol. Oceanogr. **40**: 428–433. doi:10.4319/lo.1995.40.2.0428

Coban-Yildiz, Y., M. A. Altabet, A. Yilmaz, and S. Tugrul. 2006. Carbon and nitrogen isotopic ratios of suspended particulate organic matter (SPOM) in the Black Sea water column. Deep-Sea Res. Part II Top. Stud. Oceanogr. **53**: 1875–1892. doi:10.1016/j.dsr2.2006.03.021

Codispoti, L. 2007. An oceanic fixed nitrogen sink exceeding 400 Tg N vs the concept of homeostasis in the fixed-nitrogen inventory. Biogeosciences **4**: 233–253. doi:10.5194/bg-4-233-2007

Dabundo, R., M. F. Lehmann, L. Treibergs, C. R. Tobias, M. A. Altabet, P. H. Moisander, and J. Granger. 2014. The contamination of commercial $^{15}N_2$ gas stocks with ^{15}N-labeled nitrate and ammonium and consequences for nitrogen fixation measurements. PLoS One **9**: e110335. doi:10.1371/journal.pone.0110335

Dekaezemacker, J., S. Bonnet, O. Grosso, T. Moutin, M. Bressac, and D. G. Capone. 2013. Evidence of active dinitrogen fixation in surface waters of the eastern tropical South Pacific during El Niño and La Niña events and evaluation of its potential nutrient controls. Global Biogeochem. Cycles **27**: 768–779. doi:10.1002/gbc.20063

Dickson, M. L., and P. A. Wheeler. 1993. Chlorophyll *a* concentrations in the North Pacific: Does a latitudinal

gradient exist? Limnol. Oceanogr. **38**: 1305–1330. doi:10.4319/lo.1993.38.8.1813

Dickson, M. L., and P. A. Wheeler. 1995. Reply to the note by Chavez et al. Limnol. Oceanogr. **40**: 434–436. doi:10.4319/lo.1995.40.2.0434

Dugdale, R., V. Dugdale, J. Neess, and J. Goering. 1959. Nitrogen fixation in lakes. Science **130**: 859–860. doi:10.1126/science.130.3379.859

Dunbar, R. B. 2016. Carbon chemistry (TCO_2, TALK, POC, PON, δC^{13}POM, δN^{15}POM) from CTD bottles from RVIB Nathaniel B. Palmer cruise NBP1302 in the Ross Sea, Antarctica from February to March 2013 (TRACERS project), edited. Biological and Chemical Oceanography Data Management Office. http://lod.bco-dmo.org/id/dataset/658394

Emerson, S., C. Stump, D. Wilbur, and P. Quay. 1999. Accurate measurement of O_2, N_2, and Ar gases in water and the solubility of N_2. Mar. Chem. **64**: 337–347. doi:10.1016/S0304-4203(98)00090-5

Eyre, B. D., S. Rysgaard, T. Dalsgaard, and P. B. Christensen. 2002. Comparison of isotope pairing and N_2: Ar methods for measuring sediment denitrification—Assumption, modifications, and implications. Estuaries **25**: 1077–1087. doi:10.1007/BF02692205

Farnelid, H., M. Bentzon-Tilia, A. F. Andersson, S. Bertilsson, G. Jost, M. Labrenz, K. Jürgens, and L. Riemann. 2013. Active nitrogen-fixing heterotrophic bacteria at and below the chemocline of the central Baltic Sea. J. ISME. **7**: 1413–1423. doi:10.1038/ismej.2013.26

Fernandez, C., L. Farías, and O. Ulloa. 2011. Nitrogen fixation in denitrified marine waters. PLoS One **6**: e20539. doi:10.1371/journal.pone.0020539

Ferrari, G. M., and S. Tassan. 1996. Use of the 0.22 μm Millipore membrane for light transmission measurements of aquatic particles. J. Plankton Res. **18**: 1261–1267. doi:10.1093/plankt/18.7.1261

Garçon, M., L. Sauzéat, R. W. Carlson, S. B. Shirey, M. Simon, V. Balter, and M. Boyet. 2017. Nitrile, latex, neoprene and vinyl gloves: A primary source of contamination for trace element and Zn isotopic analyses in geological and biological samples. Geostand. Geoanal. Res. **41**: 367–380. doi:10.1111/ggr.12161

Glibert, P. M., and D. A. Bronk. 1994. Release of dissolved organic nitrogen by marine diazotrophic cyanobacteria, *Trichodesmium* spp. Appl. Environ. Microbiol. **60**: 3996–4000. doi:10.1128/AEM.60.11.3996-4000.1994

Goldman, J. C., and M. R. Dennett. 1985. Susceptibility of some marine phytoplankton species to cell breakage during filtration and post-filtration rinsing. J. Exp. Mar. Biol. Ecol. **86**: 47–58. doi:10.1016/0022-0981(85)90041-3

Gradoville, M. R., D. Bombar, B. C. Crump, R. M. Letelier, J. P. Zehr, and A. E. White. 2017. Diversity and activity of nitrogen-fixing communities across ocean basins. Limnol. Oceanogr. **62**: 1895–1909. doi:10.1002/lno.10542

Granger, J. 2019. N_2 exetainer fill video. Available from https://youtu.be/18K_LtT3M4Y. Last accessed 1 March 2020.

Großkopf, T., and others. 2012. Doubling of marine dinitrogen-fixation rates based on direct measurements. Nature **488**: 361. doi:10.1038/nature11338

Grosse, J., D. Bombar, H. N. Doan, L. N. Nguyen, and M. Voss. 2010. The Mekong River plume fuels nitrogen fixation and determines phytoplankton species distribution in the South China Sea during low and high discharge season. Limnol. Oceanogr. **55**: 1668–1680. doi:10.4319/lo.2010.55.4.1668

Gruber, N. 2008. The marine nitrogen cycle: Overview and challenges, p. 1–50. *In* Capone, D. G., D. A. Bronk, M. R. Mullholand, and A. J. Carpenter [eds.], Nitrogen in the marine environment, v. 2nd ed. Academic Press, Elsevier.

Gruber, N., and J. L. Sarmiento. 1997. Global patterns of marine nitrogen fixation and denitrification. Global Biogeochem. Cycles **11**: 235–266. doi:10.1029/97GB00077

Hamersley, M. R., K. A. Turk, A. Leinweber, N. Gruber, J. P. Zehr, T. Gunderson, and D. G. Capone. 2011. Nitrogen fixation within the water column associated with two hypoxic basins in the Southern California Bight. Aquat. Microb. Ecol. **63**: 193–205. doi:10.3354/ame01494

Hamme, R. C., and S. R. Emerson. 2004. The solubility of neon, nitrogen and argon in distilled water and seawater. Deep-Sea Res. Part I Oceanogr. Res. Pap. **51**: 1517–1528. doi:10.1016/j.dsr.2004.06.009

Hannides, C. C., B. N. Popp, C. A. Choy, and J. C. Drazen. 2013. Midwater zooplankton and suspended particle dynamics in the North Pacific Subtropical Gyre: A stable isotope perspective. Limnol. Oceanogr. **58**: 1931–1946. doi:10.4319/lo.2013.58.6.1931

Hayes, J. 2004. An introduction to isotopic calculations, p. 18. Woods Hole Oceanographic Institution.

IOCCG Protocol Series. 2019. Particulate organic carbon sampling and measurement protocols: Consensus towards future ocean color missions. *In* Chaves, J. E. & others. [eds.], IOCCG Optics & Biogeochemistry Protocols for Satellite Ocean Colour Sensor Validation, Volume 6.0, IOCCG.

Jayakumar, A., B. X. Chang, B. Widner, P. Bernhardt, M. R. Mulholland, and B. B. Ward. 2017. Biological nitrogen fixation in the oxygen-minimum region of the eastern tropical North Pacific Ocean. ISME J. **11**: 2356. doi:10.1038/ismej.2017.97

Jensen, K. M., M. H. Jensen, and E. Kristensen. 1996. Nitrification and denitrification in Wadden Sea sediments (Königshafen, Island of Sylt, Germany) as measured by nitrogen isotope pairing and isotope dilution. Aquat. Microb. Ecol. **11**: 181–191. doi:10.3354/ame011181

Kana, T. M., C. Darkangelo, M. D. Hunt, J. B. Oldham, G. E. Bennett, and J. C. Cornwell. 1994. Membrane inlet mass spectrometer for rapid high-precision determination of N_2, O_2, and Ar in environmental water samples. Anal. Chem. **66**: 4166–4170. doi:10.1021/ac00095a009

Karl, D. M., R. R. Bidigare, and R. M. Letelier. 2001. Long-term changes in plankton community structure and productivity

in the North Pacific Subtropical Gyre: The domain shift hypothesis. Deep-Sea Res. Part II Top. Stud. Oceanogr. **48**: 1449–1470. doi:10.1016/S0967-0645(00)00149-1

Klawonn, I., G. Lavik, P. Böning, H. Marchant, J. Dekaezemacker, W. Mohr, and H. Ploug. 2015. Simple approach for the preparation of $^{15-15}N_2$-enriched water for nitrogen fixation assessments: Evaluation, application and recommendations. Front. Microbiol. **6**: 769. doi:10.3389/fmicb.2015.00769

Knapp, A. N., K. L. Casciotti, W. G. Berelson, M. G. Prokopenko, and D. G. Capone. 2016. Low rates of nitrogen fixation in eastern tropical South Pacific surface waters. Proc. Natl. Acad. Sci. U. S. A. **113**: 4398–4403. doi:10.1073/pnas.1515641113

Landry, M. 2014. Concentrations and stable isotope abundances of particulate organic carbon (POC) and particulate organic nitrogen (PON) from Niskin bottle samples taken on R/V Melville cruise MV1008 in the Costa Rica Dome in 2010 (CRD FLUZiE project), edited. Biological and Chemical Oceanography Data Management Office. doi:10.1575/1912/bco-dmo.516142.1

Laughlin, R. J., and R. J. Stevens. 2003. Changes in composition of nitrogen-15-labeled gases during storage in septum-capped vials. Soil Sci. Soc. Am. J. **67**: 540–543. doi:10.2136/sssaj2003.5400

Li, W. K. W. 1986. Experimental approaches to field measurements: Methods and interpretation. Can. Bull. Fish. Aquat. Sci. **214**: 251–286.

Luo, Y. W., and others. 2012. Database of diazotrophs in global ocean: Abundances, biomass and nitrogen fixation rates. Earth Syst. Sci. Data Discuss. **5**: 47–106. doi:10.5194/essdd-5-47-2012

MacDougall, D., and W. B. Crummett. 1980. Guidelines for data acquisition and data quality evaluation in environmental chemistry. Anal. Chem. **52**: 2242–2249. doi:10.1021/ac50064a004

Mahaffey, C., A. F. Michaels, and D. G. Capone. 2005. The conundrum of marine N_2 fixation. Am. J. Sci. **305**: 546–595. doi:10.2475/ajs.305.6-8.546

Makela, S., M. Yazdanpanah, I. Adatia, and G. Ellis. 1997. Disposable surgical gloves and pasteur (transfer) pipettes as potential sources of contamination in nitrite and nitrate assays. Clin. Chem. **43**: 2418–2420. doi:10.1093/clinchem/43.12.2418

Mariotti, A. 1983. Atmospheric nitrogen is a reliable standard for natural ^{15}N abundance measurements. Nature **303**: 685–687. doi:10.1038/303685a0

Matrai, P. A., and M. V. Orellana. 2012. Biology and chemistry in Arctic surface microlayer and subsurface waters from R/V Oden cruise ASCOS2008 from the High Arctic Ocean in 2008 (87° N, 1-6° E) (Marine Microgels project). Biological and Chemical Oceanography Data Management Office. http://lod.bco-dmo.org/id/dataset/3593

Merritt, D. A., and J. M. Hayes. 1994. Factors controlling precision and accuracy in isotope-ratio-monitoring mass spectrometry. Anal. Chem. **66**: 2336–2347.

Michaels, A. F., and others. 1994. Seasonal patterns of ocean biogeochemistry at the US JGOFS Bermuda Atlantic time-series study site. Deep-Sea Res. Part I Oceanogr. Res. Pap. **41**: 1013–1038. doi:10.1016/0967-0637(94)90016-7

Mohr, W., T. Grosskopf, D. W. Wallace, and J. LaRoche. 2010. Methodological underestimation of oceanic nitrogen fixation rates. PLoS One **5**: e12583. doi:10.1371/journal.pone.0012583

Moisander, P. H., R. A. Beinart, I. Hewson, A. E. White, K. S. Johnson, C. A. Carlson, J. P. Montoya, and J. P. Zehr. 2010. Unicellular cyanobacterial distributions broaden the oceanic N_2 fixation domain. Science **327**: 1512–1514. doi:10.1126/science.1185468

Moisander, P. H., A. E. White, and J. Granger. 2019. EAGER: Collaborative research: Detection limit in marine nitrogen fixation measurements – constraints from the mesopelagic ocean. Biological and Chemical Oceanography Data Management Office. doi:10.1575/1912/bco-dmo.778000.1

Montoya, J. P. 2008. Chapter 29: Nitrogen stable isotopes in marine environments. p. 1277–1293. *In* Capone, D. G., D. A. Bronk, M. R. Mulholland, and E. J. Carpenter [eds.], Nitrogen in the marine environment, 2nd ed. Elsevier.

Montoya, J. P., M. Voss, P. Kahler, and D. G. Capone. 1996. A simple, high-precision, high-sensitivity tracer assay for N_2 fixation. Appl. Environ. Microbiol. **62**: 986–993. doi:10.1128/AEM.62.3.986-993.1996

Morán, X. A. G., J. M. Gasol, L. Arin, and M. Estrada. 1999. A comparison between glass fiber and membrane filters for the estimation of phytoplankton POC and DOC production. Mar. Ecol. Prog. Ser. **187**: 21–41.

Mulholland, M. R., and others. 2012. Rates of dinitrogen fixation and the abundance of diazotrophs in North American coastal waters between Cape Hatteras and Georges Bank. Limnol. Oceanogr. **57**: 1067–1083. doi:10.4319/lo.2012.57.4.1067

Mulholland, M. R., P. W. Bernhardt, B. N. Widner, C. R. Selden, P. D. Chappell, S. Clayton, A. Mannino, and K. Hyde. 2019. High rates of N_2 fixation in temperate, western North Atlantic coastal waters expand the realm of marine diazotrophy. Global Biogeochem. Cycles. **33**: 826–840. doi:10.1029/2018GB006130

Nayar, S., and L. M. Chou. 2003. Relative efficiencies of different filters in retaining phytoplankton for pigment and productivity studies. Estuar. Coast. Shelf Sci. **58**: 241–248. doi:10.1016/S0272-7714(03)00075-1

N-Fixation Working Group. 2019a. Metadata: ^{15}N tracer incubations for N_2 fixation measurements. Ocean Carbon Biogeochemistry. Available from https://www.us-ocb.org/n-fixation-working-group/. Last accessed 1 March 2020.

N-Fixation Working Group. 2019b. $^{15}N_2$ contaminant database. Ocean Carbon Biogeochemistry. Available from https://www.us-ocb.org/n-fixation-working-group/. Last accessed 1 March 2020.

N-Fixation Working Group. 2019c. Relevant documents - spreadsheet. Ocean Carbon Biogeochemistry. Available from https://www.us-ocb.org/n-fixation-working-group/. Last accessed 1 March 2020.

Novak, M. G., I. Cetinić, J. E. Chaves, and A. Mannino. 2018. The adsorption of dissolved organic carbon onto glass fiber filters and its effect on the measurement of particulate organic carbon: A laboratory and modeling exercise. Limnol. Oceanogr. Meth. **16**: 356–366. doi:10.1002/lom3.10248

Oczkowski, A., B. Kreakie, R. A. McKinney, and J. Prezioso. 2016. Patterns in stable isotope values of nitrogen and carbon in particulate matter from the Northwest Atlantic continental shelf, from the Gulf of Maine to Cape Hatteras. Front. Mar. Sci. **3**: 252. doi:10.3389/fmars.2016.00252

Phinney, D. A., and C. S. Yentsch. 1985. A novel phytoplankton chlorophyll technique: Toward automated analysis. J. Plankton Res. **7**: 633–642. doi:10.1093/plankt/7.5.633

Platt, T. G., C. L. Gallegos, and W. G. Harrison. 1981. Photoinhibition of photosynthesis in natural assemblages of marine phytoplankton. J. Marine Res. **38**: 687–701.

Rahav, E., E. Bar-Zeev, S. Ohayion, H. Elifantz, N. Belkin, B. Herut, M. R. Mulholland, and I. R. Berman-Frank. 2013. Dinitrogen fixation in aphotic oxygenated marine environments. Front. Microbiol. **4**: 1–11.

Révész, K., H. Qi, and T.B. Coplen. 2012. Determination of the $\delta^{15}N$ and $\delta^{13}C$ of total nitrogen and carbon in solids; RSIL lab code 1832, chap. 5 *of* Stable isotope-ratio methods, sec. C *of* Révész, K, and Coplen, T.B. [eds.], Methods of the Reston Stable Isotope Laboratory (slightly revised from version 1.1 released in 2007): U.S. Geological Survey Techniques and Methods, book 10, p. 31. Available from https://pubs.usgs.gov/tm/2006/tm10c5/

Ripp, J. 1996. Analytical detection limit guidance & laboratory guide for determining method detection limits. Wisconsin Department of Natural Resources, Laboratory Certification Program.

Selden, C. R., M. R. Mulholland, P. W. Bernhardt, B. Widner, A. Macías-Tapia, Q. Ji, and A. Jayakumar. 2019. Dinitrogen fixation across physico-chemical gradients of the Eastern Tropical North Pacific oxygen deficient zone. Global Biogeochem. Cycles **33**: 1187–1202. doi:10.1029/2019GB006242

Sharp, Z. 2017. Principles of stable isotope geochemistry, 2nd ed. University of New Mexico Digital Repository. doi:10.25844/h9q1-0p82

Sipler, R. E., D. Gong, S. E. Baer, M. P. Sanderson, Q. N. Roberts, M. R. Mulholland, and D. A. Bronk. 2017. Preliminary estimates of the contribution of Arctic nitrogen fixation to the global nitrogen budget. Limnol. Oceanogr.: Lett. **2**: 159–166. doi:10.1002/lol2.10046

Smith, R., C. Tobias, P. Vlahos, C. Cooper, M. Ballentine, and T. Ariyarathna. 2015. Mineralization of RDX-derived nitrogen to N_2 via denitrification in coastal marine sediments. Environ. Sci. Technol. **49**: 2180–2187. doi:10.1021/es505074v

Struempler, A. W. 1973. Adsorption characteristics of silver, lead, cadmium, zinc, and nickel on borosilicate glass, polyethylene, and polypropylene container surfaces. Anal. Chem. **45**: 2251–2254. doi:10.1021/ac60335a014

Sturm, K., B. Keller-Lehmann, U. Werner, K. R. Sharma, A. R. Grinham, and Z. Yuan. 2015. Sampling considerations and assessment of Exetainer usage for measuring dissolved and gaseous methane and nitrous oxide in aquatic systems. Limnol. Oceanogr. Methods **13**: 375–390. doi:10.1002/lom3.10031

Taguchi, S., and E. A. Laws. 1988. On the microparticles which pass through glass-fiber filter type GF/F in coastal and open waters. J. Plankton Res. **10**: 999–1008. doi:10.1093/plankt/10.5.999

Tang, W., and others. 2019. Revisiting the distribution of oceanic N_2 fixation and estimating diazotrophic contribution to marine production. Nat. Commun. **10**: 83. doi:10.1038/s41467-019-08640-0

Thompson, A. W., and others. 2012. Unicellular cyanobacterium symbiotic with a single-celled eukaryotic alga. Science **337**: 1546–1550. doi:10.1126/science.1222700

Turk-Kubo, K. A., H. M. Farnelid, I. N. Shilova, B. Henke, and J. P. Zehr. 2017. Distinct ecological niches of marine symbiotic N_2-fixing cyanobacterium *Candidatus Atelocyanobacterium thalassa* sublineages. J. Phycol. **53**: 451–461. doi:10.1111/jpy.12505

Turk-Kubo, K. A., M. Karamchandani, D. G. Capone, and J. P. Zehr. 2014. N_2-fixing potential of heterotrophs in the ETSP. Environ. Microbiol. **16**: 3095–3114. doi:10.1111/1462-2920.12346

Turnewitsch, R., and others. 2007. Determination of particulate organic carbon (POC) in seawater: The relative methodological importance of artificial gains and losses in two glass-fiber-filter-based techniques. Mar. Chem. **105**: 208–228. doi:10.1016/j.marchem.2007.01.017

Wannicke, N., M. Benavides, T. Dalsgaard, J. W. Dippner, J. P. Montoya, and M. Voss. 2018. New perspectives on nitrogen fixation measurements using $^{15}N_2$ gas. Front. Mar. Sci. **5**: 120. doi:10.3389/fmars.2018.00120

Weiss, R. 1970. The solubility of nitrogen, oxygen and argon in water and seawater. Deep Sea Res. Oceanogra. Abstracts **17**: 721–735. doi:10.1016/0011-7471(70)90037-9

White, A. E., R. A. Foster, C. R. Benitez-Nelson, P. Masqué, E. Verdeny, B. N. Popp, K. E. Arthur, and F. G. Prahl. 2013. Nitrogen fixation in the Gulf of California and the Eastern Tropical North Pacific. Prog. Oceanogr. **109**: 1–17. doi:10.1016/j.pocean.2012.09.002

Wilson, S. T., D. Böttjer, M. J. Church, and D. M. Karl. 2012. Comparative assessment of nitrogen fixation methodologies,

conducted in the oligotrophic North Pacific Ocean. Appl. Environ. Microbiol. **78**: 6516–6523. doi:10.1128/AEM.01146-12

Yentsch, C. S. 1983. A note on the fluorescence characteristics of particles that pass through glass-fiber filters. Limnol. Oceanogr. **28**: 597–599. doi:10.4319/lo.1983.28.3.0597

Zehr, J. P., M. T. Mellon, and S. Zani. 1998. New nitrogen-fixing microorganisms detected in oligotrophic oceans by amplification of nitrogenase (*nifH*) genes. Appl. Environ. Microbiol. **64**: 3444–3450. doi:10.1128/AEM.64.9.3444-3450.1998

Zehr, J. P., and P. J. Turner. 2001. Nitrogen fixation: Nitrogenase genes and gene expression, p. 271–286. *In* J. H. Paul [ed.], Methods in microbiology v. **30**. Academic Press, Elsevier.

Zehr, J. P., S. R. Bench, B. J. Carter, I. Hewson, F. Niazi, T. Shi, H. J. Tripp, and J. P. Affourtit. 2008. Globally distributed uncultivated oceanic N_2-fixing cyanobacteria lack oxygenic photosystem II. Science **322**: 1110–1112. doi:10.1126/science.1165340

Acknowledgments

This work was supported by a collaborative NSF EAGER grant to P.M. (OCE-1733610), J.G. (OCE-1736659), and A.E.W. (OCE-1732206) and a workshop supported by the Ocean Carbon & Biogeochemistry (OCB) program. We thank Brittany Widner for insights on detection limits, and Holly Westbrook for technical assistance. We also acknowledge the Hawaii Ocean Time-series program for support and access to the sea aboard HOT 312. Data from this work are archived with BCO-DMO (Moisander et al. 2019).

Conflict of Interest

None declared.

Submitted 29 May 2019
Revised 26 November 2019
Accepted 03 February 2020

Associate editor: Ben Surridge